University of South-Eastern Norway
Faculty of Health and Social Sciences

Master's Thesis

Study programme: MSc Optometry and Visual Science (Orthoptics and Paediatric Optometry)

Spring 2020

Issah Imoro

Non-invasive Raman spectroscopy of Albumin in the aqueous humor of the anterior chamber of the eye

An initial in vitro validation of a novel slit lamp mounted setup for Raman spectroscopy of proteins in the aqueous humor of the living eye using a customized eye model

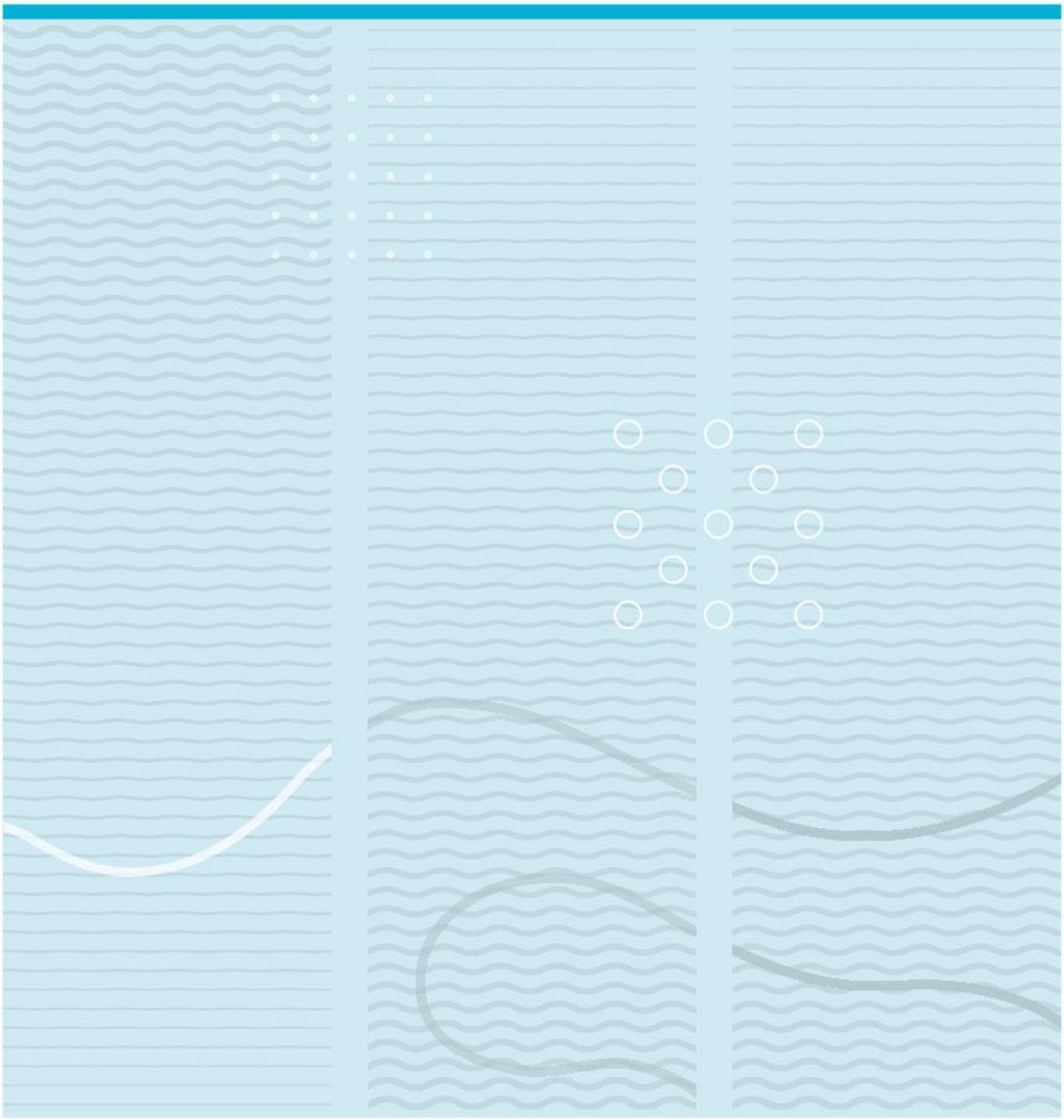

University of South-Eastern Norway
Faculty of Health and Social Sciences
Department of Optometry, Radiography and Lighting Design
PO Box 235
NO-3603 Kongsberg, Norway

http://www.usn.no

This thesis is worth 30 study points

Summary

Introduction:

Aqueous humor proteins have been identified as important biomarkers for ocular diseases. The main aim of this study was to perform an initial in vitro validation of a novel patented instrumental setup for non-invasive measurements of proteins in the aqueous humor of the anterior chamber of the human eye by means of an adapted Raman spectrometer mounted to a commercial slit lamp microscope.

Methods:

We used Bovine Serum Albumin (BSA) and a model eye for measurements with Raman spectroscopy: Twenty-five measurements related to the number of samples to obtain a noise cancelling effect on the Raman shift intensity, five related to repeatability, sixteen related to linearity and concentrations of Albumin within a physiologic range (i.e. 0.02 - 2.08 mg/ml). Spectral data preprocessing included a smoothing Savitsky-Golay of a polynomial order 2 and 3 smoothing points followed by a standard normal variate transformation for baseline correction and normalization. Principal component analysis with full cross validation and partial least square regression were run on the data to establish the predictive ability of the model.

Results:

Simulations showed that noise was sufficiently cancelled with twelve samples. The coefficient of variation was determined as 0.69 % indicating an excellent repeatability of the measurements in 1650 cm^{-1} band. Partial least square regression showed the ability of the patented instrumental setup to measure low concentrations of Albumin in the physiologic range down to 0.2 mg/ml with increasing certainty of linearity as the concentration increases.

Conclusion:

The results of the study have for the first time shown that a novel patented instrumental setup for Raman spectroscopy of the molecular content of the aqueous humor is able to provide measurements of Albumin at physiologic concentrations with a high degree of linearity and repeatability from a model eye.

Key words: Biomarkers, Raman, Spectroscopy, Albumin

Contents

Acknowledgement

First and foremost, I wish to thank God for granting me sound health and the strength to successfully complete this work. Secondly, I wish to extend sincere gratitude to my supervisor Per Olof Lundmark (PhD) (University of South-Eastern Norway) for providing me very constant and timely advice during this work. His patience and excellent feedback were very crucial to the successful completion of this thesis. My thanks also go to Professor Jan Richard Bruenech (University of South-Eastern Norway), Martin Larsen Medical As (Kongsberg, Norway) and Jon Tschudi (SINTEF Oslo) for their contributions to this work. Thanks also go to statistician Tor Martin Kvikstad for his help in developing a simulation model. I wish to also thank the program coordinators Trine Langaas (PhD) and Helle Kristine Falkenberg (PhD) for always being there to pass out relevant information. I thank the entire management of the University of South-Eastern Norway for granting me the opportunity to study in this prestigious University.

I would also like to thank my parents Imoro Wuni and Binta Musah, my wife Amina Salifu and son Humayd Zanya Issah for their prayers and support throughout my studies. Though being far away, their constant love, patience and sacrifice were my major source of motivation throughout my study period in Norway.

Oslo, May 2020
Issah Imoro

1 Introduction

Proteins are large biological molecules consisting of one or more long chains of amino acid residues and they perform several functions within living organisms including catalysing metabolic reactions, replicating Deoxyribonucleic acid (DNA), responding to stimuli, and transporting molecules from one location to another (Aboul-Enein & Hoang, 2015). Proteins are distinguished from one another by their amino acid sequence and this is directed by their gene nucleotide sequence resulting in the wrapping of the protein into a specific three-dimensional structure that determines its activity (Aboul-Enein & Hoang, 2015).

The term “proteomics” which refers to the analysis of the entire protein content of a cell, tissue, or organism under a specific, defined set of conditions was first used by Marc Wilkins in 1996 to describe what he referred to as the “PROTein complement of a genOME“ (Wilkins et al., 1996). Proteomics has a vital role in the characterization of proteins, including their expression, structure, functions, interactions and modifications (Domon & Aebersold, 2006). Proteomics has been described as a crucial process for early disease diagnosis, prognosis as well as in monitoring disease development and it is also regarded as playing a vital role in the pharmaceutical industry (Aslam, Basit, Nisar, Khurshid, & Rasool, 2017).

Several methods have been designed to be used in the analysis of proteins. Enzyme-linked immunosorbent assay (ELISA) and western blotting methods are most often used to analyse few selected proteins (Aslam et al., 2017). Sodium dodecyl sulphate-polyacrylamide gel electrophoresis (SDS-PAGE), two-dimensional gel electrophoresis (2-DE) and two-dimensional differential gel electrophoresis (2D-DIGE) techniques are used for the separation of complex protein samples (Dunn, 1986). Another technique is protein microarrays or chips that have been developed for high-throughput and rapid analysis (Aslam et al., 2017). Other methods with high sensitivity include mass spectroscopy, nuclear magnetic resonance (NMR) spectroscopy (Wiese, Reidegeld, Meyer, & Warscheid, 2007) and Raman Spectroscopy which will be discussed in detail in section 1.1.

1.1 Spectroscopic analysis and Raman principle

Spectroscopy is the study of interaction of electromagnetic radiation with matter (Bumbrah & Sharma, 2016). A number of spectroscopic methods are based on phenomena of emission, absorption, fluorescence or scattering and are applied in different kinds of studies based on the major purpose of the analysis (Settle, 1997). These methods are utilized for both qualitative and quantitative analysis of samples (analytes) (Bumbrah & Sharma, 2016). Qualitative analysis is performed to establish the identity of a sample while quantitative analysis is performed to estimate the concentration of an analyte in a given sample (Settle, 1997).

Spectroscopic methods vary based on the portion of the electromagnetic spectrum (figure 1) used in excitation. For instance the ultra-violet (UV) portion of the electromagnetic spectrum can be used as a screening for the identification of samples whereas techniques like infrared spectroscopy are used as confirmatory methods since they provide a reliable identity of sample and are unique in nature (Willard, Meritt, Dean, & Settle, 1988). Other spectroscopic methods use different radiation wavelengths of the electromagnetic spectrum.

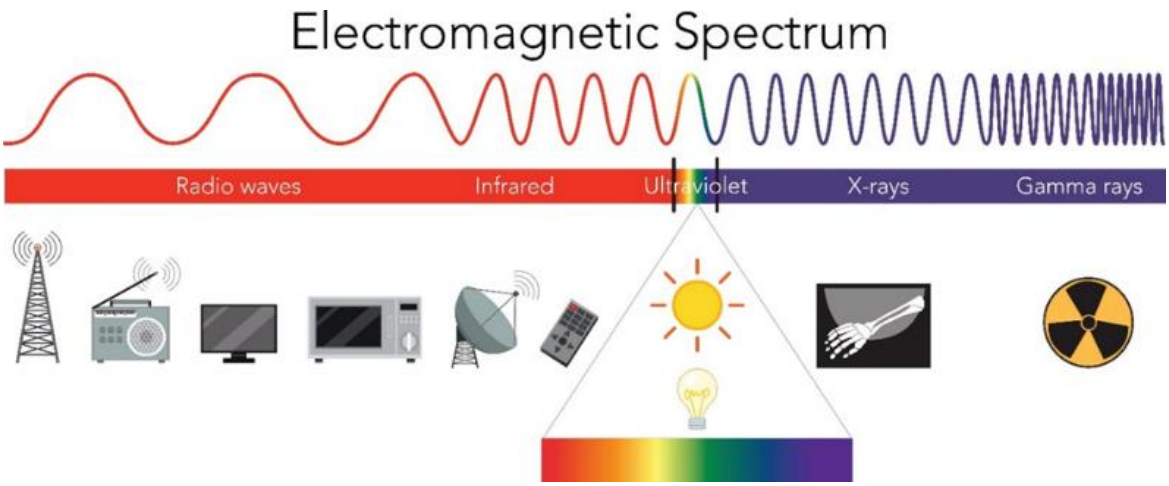

Figure 1: Illustration of the electromagnetic spectrum showing the different portions used in spectroscopic analysis. Image courtesy: (Colourbox, 2020) Royalty free

The Raman effect or phenomenon, which is applied in Raman Spectroscopy, was remarkably discovered by the Indian scientist Sir Chandrasekhra Venkata Raman in 1928 with very little instrumentation (figure 2) when he used sunlight as a source of light, a telescope as the collector

and his eyes as detector (Ferraro, Nakamoto, & Brown, 2003). The phenomenon is basically described as the inelastic scattering of light that falls on an object and this is described in further detail in section 1.1.1. This phenomenon for which he won the Nobel prize in Physics in 1930 (Nobel Prize, 2020) can be used for qualitative analysis by measuring frequency of scattered radiations and for quantitative analysis by measuring the intensity of scattered radiations (Willard et al., 1988).

Permission not received at time of submission, so image was not included

Figure 2: A picture of Sir C. V. Raman with the quartz spectrograph used to measure the wavelengths of the scattered light that became known as the Raman Effect. Photo courtesy: (American Chemical Society, 1998).

1.1.1 Principle of Raman spectroscopy

When light strikes a surface, it is either absorbed, transmitted or scattered (Ikeuchi & Sato, 1991). The Raman effect is based on the principle of inelastic scattering of light (Chalmers, Edwards, & Hargreaves, 2012) which means the frequency of a small fraction of the scattered radiation is different from the frequency of the monochromatic (i.e. having the same wavelength) incident radiation (Bumbrah & Sharma, 2016). This small fraction of scattered radiation which constitutes inelastic scattering of the incident radiation is different from the elastic scattering also called Rayleigh scattering of light in which the scattered radiation has an equal frequency to the incident monochromatic radiation (Bumbrah & Sharma, 2016). Thus, in Raman spectroscopy, a sample is illuminated with a monochromatic laser beam which interacts with the molecules of the sample and generates scattered light which is inelastic, and this is used to construct a Raman spectrum (figure 3) (Bumbrah & Sharma, 2016).

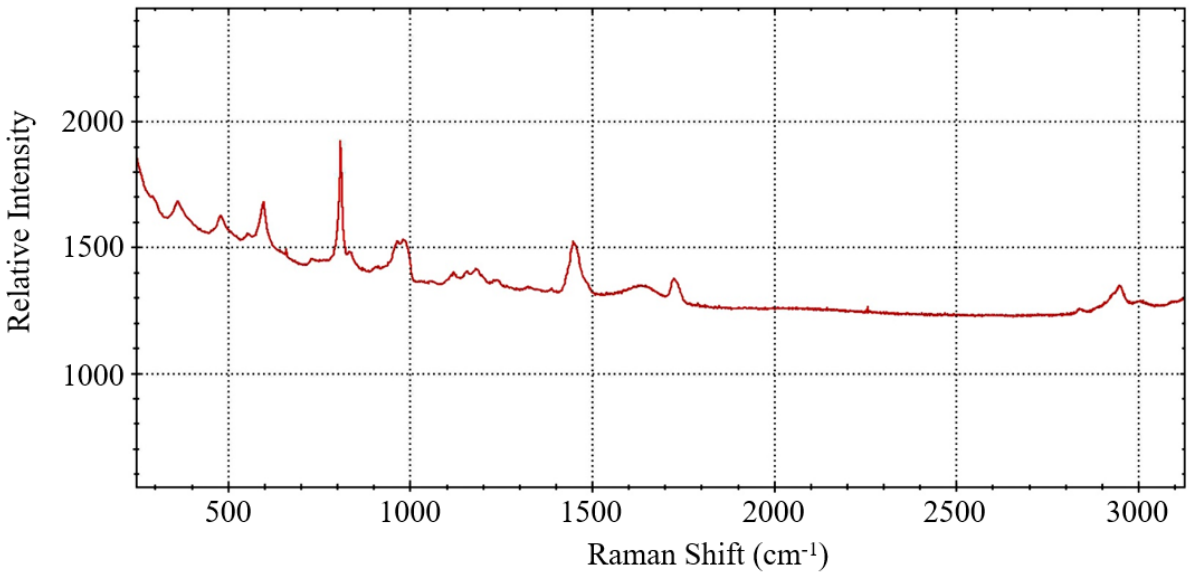

Figure 3: Results from Raman spectroscopy of a sample with low protein concentration. The bands in the spectrum are identified by unique wavenumbers. The x-axis provides a "fingerprint" of the protein composition and the height of the bands reflects the protein's concentration (from a pilot study at SINTEF, Oslo)

The Raman spectrum is presented as an intensity-versus-wavenumbers (Raman shift) with units of cm^{-1} and is usually recorded over a range of 4000 - 10 cm^{-1} (Bumbrah & Sharma, 2016). From the horizontal axis, the wavenumbers give molecular vibration information used to identify the analyte/sample (i.e. the substance whose chemical constituents are being identified and measured). The vertical axis of the spectrum represented by the intensity gives the strength of activity and it is used to estimate the concentration of the analyte (Nano Photon, 2020). In spectroscopy, the wavenumber is described as a unit that represents the frequency of radiation presented as the reciprocal of the wavelength in centimetres (Harrison, 2009). Wavenumber has been the historic unit in spectroscopy (Tkachenko, 2006) and it is used instead of frequency because it allows for easy comparison of values since it is regarded as a unit of energy. The spectral band described in figure 3 is produced when a radiation on a molecular bond of a sample at a specific frequency vibrates and it is defined by three parameters namely location (specified by the wavenumber), height (specified by the intensity) and width (Burns & Ciurczak, 2007).

Figure 4 illustrates the three possible outcomes from the scattering of light. From left to right, Rayleigh scattering is depicted by a blue arrow representing excitation light and a black arrow as scattered light with an equal length of the arrows indicating equality in the respective energies of the excitation and scattered lights. In the case of Stokes Raman scattering, the scattered light represented by the green arrow has a lower energy depicted by a shorter length of the arrow as compared to the excitation light. For Anti-Stokes Raman scattering, the scattered light represented by the purple arrow has a higher energy depicted by a longer length of its arrow as compared to the excitation light. The difference in width of arrows was used to distinguish between the 3 types of scattering in the diagram.

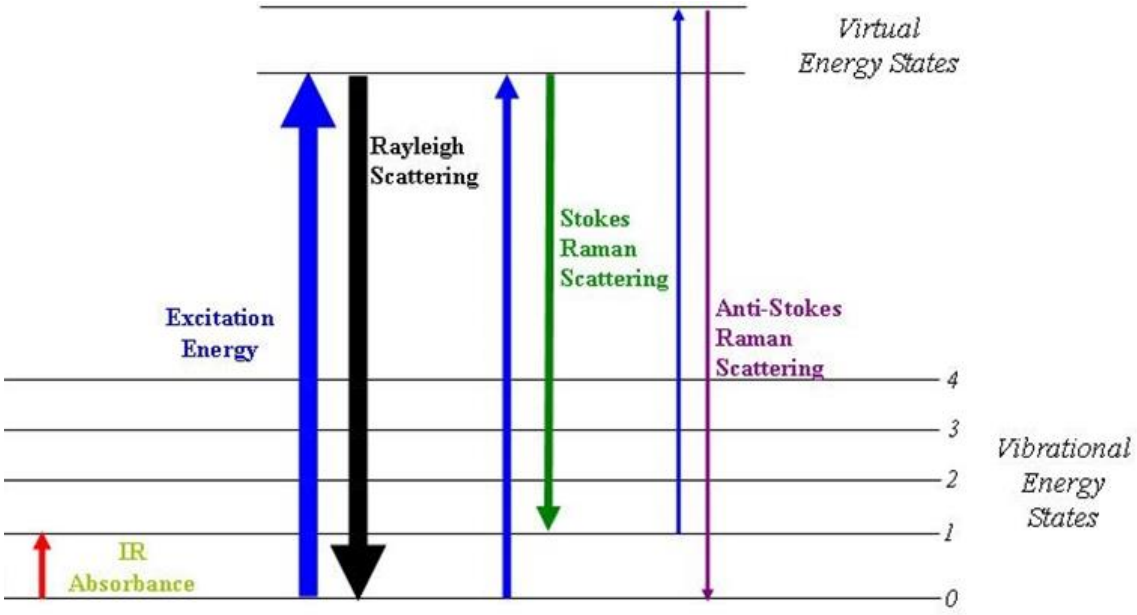

Figure 4: Presentation of Rayleigh, Stokes and Anti-Stokes scattering showing the difference in energy between excitation light and scattered light. Image courtesy: (Pavlina2.0, 2006) and reproduced with license CC-BY-SA 2.5

The Raman shift indicated on the x-axis of the spectrum (figure 3) is the numeric representation of the energy difference between the initial and final energy levels resulting from the difference in wavelength as indicated in the figure 4 above and it is represented by the mathematical formula:

$$\Delta v = \left(\frac{1}{\lambda 0}\right) - \left(\frac{1}{\lambda 1}\right) \qquad (1.1)$$

where Δv is the Raman shift expressed in wavenumber (cm^{-1}), λ0 is the excitation wavelength, and λ1 is the Raman spectrum wavelength.

If the excitation and Raman wavelengths are given in nanometers (nm), the Raman shift in cm^{-1} is obtained by the expression:

$$\Delta v = \left(\frac{1}{\lambda 0 nm}\right) - \left(\frac{1}{\lambda 1 nm}\right) x \left(10000000 \frac{nm}{cm}\right) \qquad (1.2)$$

For instance, an excitation wavelength of 785 nm in the near infrared range and a Raman wavelength of 823.8 nm (Stokes scattering) gives a Raman shift (wavenumber) of 600 cm^{-1}.

In Raman spectroscopy, the choice of wavelength of the laser source most often depends on the required application (Jones, Hooper, Zhang, Wolverson, & Valev, 2019). Shorter visible wavelengths and UV cause strong photoluminescence in organic materials and this can mask the Raman bands of the analyte (Jones et al., 2019). Photoluminescence is defined as a process in which a molecule absorbs a photon exciting one of its electrons to a higher electronic excited state, and then radiates a photon as the electron returns to a lower energy state (Munson, L.Gottfried, Jr, McNesby, & Miziolek, 2007). Thus, a major difference between photoluminescence and Raman scattering is that in photoluminescence there is absorption of the incident light first before emission of an electron whereas Raman scattering only deals with scattering of the incident light. A longer visible or near infrared (IR) wavelength (500 —830 nm) laser source is often suited for studying organic materials, because of the reduced photoluminescence that is associated with longer wavelengths (Jones et al., 2019). However, the Raman signal intensity is inversely proportional to the wavelength of the excitation light. So even though longer wavelengths are preferred for studying organic samples they require longer acquisition times (Long, 2002).

The significant regions also called fingerprint regions of the Raman spectrum that are observed within biological specimens fall within 2,000 - 400 cm^{-1} with wavenumbers for proteins falling within (1,700 – 1,500 cm^{-1}), carbohydrates (1,200 - 470 cm^{-1}), phosphate groups of DNA (980, 1,080

and 1,240 cm^{-1}) and other cellular biomolecules (Clemens, Hands, Dorling, & Baker, 2014). Furthermore, Raman spectroscopy can also be used to observe higher-frequency wavenumbers (3,500 – 2,700 cm^{-1}) that fall outside the above fingerprint region. These higher-frequency wavenumbers are often associated with Methylidyne (CH), Imidogen (NH), Hydroxide (OH) and some proteins (Movasaghi, Rehman, & Rehman, 2007).

The Raman spectroscopy setup is made up of three (3) basic components: an incident laser that provides the monochromatic light source, an optical system that focuses the light unto the sample, which also allows for sample surface observations, and a Raman spectrometer that collects the scattered light (Hou, Mougin, Ager, & Galerie, 2011). Figure 5 presents an illustration of the basic setup of a Raman experiment.

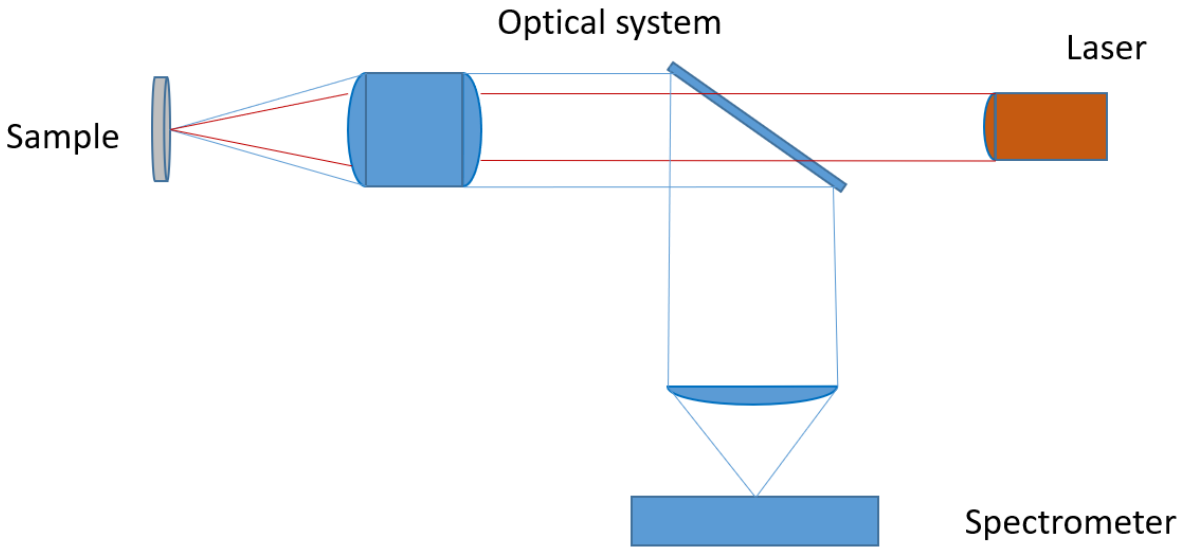

Figure 5: Illustration of a simplified Raman experimental setup showing the 3 basic components Laser source, Optical system, Raman spectrometer and a sample that is analysed.

1.2 Advantages and limitations of Raman spectroscopy

Raman spectroscopy provides an important advantage of non-invasiveness of analytes or tissues and has the ability to analyse less sample volume (Li, Kuo, & Chang, 2010). This makes it specifically suited for clinical applications (Eberhardt, Stiebing, Matthäus, Schmitt, & Popp, 2015). Furthermore, Raman spectroscopy in combination with modern optical developments is a powerful tool for potential applications in molecular diagnostics and it provides unique and specific information about the biochemical composition of analytes (Eberhardt et al., 2015).

Advantages of Raman spectroscopy for biomedical applications include being relatively fast to acquire, and it is able to provide information at the molecular level. Also, water produces weak Raman scattering, and this means the presence of water in the sample does not interfere with the spectrum of the sample that is being analysed (Ramírez-Elías & González, 2018).

Major limitations of Raman spectroscopy include weak Raman signals and undesirable noise sources such as the intense photoluminescence present in biological samples (Ramírez-Elías & González, 2018). Infrared spectrum range is divided into IR - A (1400 - 760 nm), IR - B (3000 - 1400nm), and IR - C (1000’000 -3000 nm and 1000 - 3 μm) with increasing absorption in water as you move from IR - A to IR - C (Cobarg, 1995). Therefore, excitation using near infrared (NIR) which falls within the IR - A is one of the major techniques that has been employed to avoid the photoluminescence caused by biological samples that sometimes mask the weak Raman signals mentioned above (Zhao, Lui, McLean, & Zeng, 2010).

1.3 Applications of Raman spectroscopy in protein analysis and medicine

Raman spectroscopy has emerged as a useful tool for the analysis of protein and characterization of secondary structure (three dimensional form of local segments of proteins usually alpha helices and beta sheets) with a good precision (Kitagawa & Hirota, 2002). It is increasingly being used to characterize matter ranging from simple amino acids to complex structures like proteins and because it is insensitive to water, it provides an opportunity to characterize biological analytes in

solution without affecting the results, thereby preserving the biological activity of the analytes (Stewart & Fredericks, 1999).

There has been a huge rise in both the applications of Raman spectroscopy and the number of laboratories that utilize this technique in recent times. This increase has been attributed to significant advances in instrumentation, methodology, and the relatively low cost of the Raman instrumentation. Also the obvious success associated with recent applications of Raman spectroscopy has been identified as a reason for the rise in applications of the technology by several laboratories (Aboul-Enein & Hoang, 2015).

The success of Raman spectroscopy in biomedical applications has also been attributed to the difference in molecular composition between healthy tissue and diseased tissue and also because several disease biomarkers can be identified in Raman spectra. This makes it possible to be used to diagnose or monitor the progress of certain medical conditions (Ramírez-Elías & González, 2018).

Raman spectroscopy uses laser as the excitation source because lasers provide enough power to the sample in order to detect Raman spectra in a reasonable integration time. However, important factors such as power, integration time, and wavelength of the laser to optimize the Raman system for in vivo biomedical applications are relevant factors that needs to be considered to avoid complications due to laser use (Ramírez-Elías & González, 2018). As such, in order to avoid tissue damage, two important factors that need to be considered in this regard are the maximum permissible exposure to the laser and temperature increase of the light source. This makes the criteria for a suitable laser power selection to depend on a balance between achieving a good signal to noise and to minimize tissue damage (Ramírez-Elías & González, 2018).

Raman spectroscopy has several derivatives that are applied in different types of analysis. Some of these are Confocal Raman spectroscopy modified by the addition of a confocal microscope that allows depth measurements within a tissue and Coherent Anti-Stokes Raman scattering (CARS) which is modified by using multiple laser frequencies to analyse tissues. Other variants include Drop coating deposition Raman spectroscopy (DCDRS), Surface-enhanced Raman spectroscopy/scattering (SERS), Confocal Raman microscopy (CRM) and Fourier transform infrared (FTIR) spectroscopy (Butler et al., 2016).

1.3.1 Raman Spectroscopy in the Eye

There is a growing interest in using Raman spectroscopy for clinical purposes. Artemyev and colleagues (Artemyev et al., 2016) obtained and analysed human blood samples using Raman spectroscopy to look at the prominent bands associated with the plasma proteins. The major outcome of this study was that Raman spectroscopy is a viable method of quantitatively measuring the concentrations of Albumin in human blood as well as qualitatively identifying specific proteins based on the expression of the Raman bands. These findings are of importance for the future analysis of protein concentrations in human aqueous humor, which will be discussed later since aqueous humor proteins are a fraction of blood proteins.

There are several potential applications of Raman spectroscopy in the eye and visual science (Noel, Massoud, Fred, & James, 2005). A summary of the literature on how Raman spectroscopy has been applied in the eye is displayed in table 1:

Study	Medium	Method	Major findings
(Filik & Stone, 2008)	In vitro: Dried human tear film	DCDRS using 830nm diode laser	Were able to identify tear proteins, urea, bicarbonate and lipid components
(Reyes-Goddard, Barr, & Stone, 2008)	In vitro: Synthetic tear film	SERS using NIR 830nm semiconductor diode laser	Detected the presence of herpes simplex viral particles
(Pelletier, Lambert, & Borchert, 2005)	In vitro: Human aqueous humor	Raman spectrometer using Coherent Sabre argon laser 785nm	Determined glucose concentration
(Hosseini, Jongsma, Hendrikse, & Motamedi, 2003)	In vivo: Rabbit aqueous humor	CCD -based Raman spectroscopic system	Were able to detect ceftazidime and amphotericin B
(Bauer et al., 1998)	In vitro and In vivo: Rabbit Cornea	CRM using an argon laser 514.5nm	Characterized hydration of the anterior part of the cornea
(Chen, Cheng, Li, & Lin, 2006)	In vitro: Human Cornea	FTIR and CRM using 532nm laser	Identified the chemical composition of calcifications
(Siebinga et al., 1992)	In vitro: Human Lens	CRM using 660nm laser light	Found similarities in cortical proteins of 'old' and 'young' donor lenses
(Duindam, Vrensen, Otto, & Greve, 1998)	In vitro: Human Lens	CRM using 676nm laser light	Identified elevated levels of cholesterol in opacities
(Sebag, Nie, Reiser, Charles, & Yu, 1994)	In vitro: Human Vitreous	Near-IR FT using excitation at 641nm	Identified structural differences in vitreous between patients with diabetes and controls
(Gellermann & P. S. Bernstein, 2004)	In vitro: Excised human (postmortem) eye cups	Resonant excitation	Identified changes in the structure of pigments lutein and zeaxanthin
(Evans et al., 2009)	Ex vivo: Human and Porcine retina	CRM using 632.8 nm laser light	Were able to collect OCT volumetric data and biochemical Raman spectral maps simultaneously

Table 1: Summary of Raman spectroscopy applications in the eye. Abbreviations: DCDRS: Drop coating deposition Raman spectroscopy, SERS: Surface-enhanced Raman spectroscopy/scattering, CRM: Confocal Raman microscopy, FTIR: Fourier transform infrared, FT: Fourier transform, CCD: Charged coupled device

The human tear fluid has been described as a complex mixture of proteins, lipids, metabolites and electrolytes (Ohashi, Dogru, & Tsubota, 2006) and a change in the concentration of these components can impair the ability of tear fluid to perform its key functions and this mostly is a key sign of the onset of disease (Filik & Stone, 2008) . Filik and Stone (Filik & Stone, 2008) applied Raman spectroscopy for tear film component in vitro analysis. Using a fine flame-polished capillary tube, they collected non-reflex basal tear fluid from three volunteers who were all non-contact lens wearers and had been free from ocular infection for at least three years. They were able to identify tear proteins, urea, bicarbonate and lipid components in dried tear drops. Their study showed the feasibility of using Raman spectroscopy to identify proteins associated with tear film. Also, Reyes-Goddard et al (Reyes-Goddard et al., 2008) used Raman spectroscopy with NIR to analyse herpes simplex virus in synthetic tear film. They modelled the synthetic tear after the aqueous layer of the human tear to avoid tear film variability that will come from human samples and obtained heat denatured herpes simplex virus in transport medium culture from a public health laboratory. The results of their study showed good sensitivity and specificity of the Raman spectrometer in detecting the presence of viral particles in tear film. This finding re-enforces the fact that Raman spectroscopy can be used as a clinical tool in detecting diseases in ocular tissues.

In the aqueous humor, Pelletier and colleagues (Pelletier et al., 2005) used Raman spectroscopy to determine glucose concentrations of in vitro human aqueous humor samples from cataract patients. Their study showed the capability of using Raman spectroscopy to quantify the amount of biomolecules (glucose in this case) whose amount may be altered in the state of infections/disease in the human aqueous humor. Also, Hosseini and colleagues (Hosseini et al., 2003) used Raman spectroscopy to non-invasively (in vivo) detect ceftazidime and amphotericin B injected in the aqueous humor of rabbit eyes through a needle. The results of their study show the capability of Raman spectroscopy to non-invasively detect substances in the aqueous humor.

Bauer and colleague researchers (Bauer et al., 1998) used Raman spectroscopy for in vitro and in vivo evaluation of corneal water content of New Zealand white rabbits. They did this by analysing the ratio of Raman intensities of the OH-bond and the CH-bond using enucleated rabbit eyes for the in vitro studies and eyes of rabbits under anesthesia for the in vivo investigation. Their findings showed that it was possible to use Raman spectroscopy to non-invasively characterize hydration of the anterior part of the cornea. This further shows the relevance of Raman spectroscopy as a

possible clinical diagnostic tool for ocular conditions because of the successful in vivo analysis. Chen and colleagues (Chen et al., 2006) used Raman spectroscopy for in vitro analysis of calcification of human cornea excised from a 50 years old donor. Their findings proved that Raman spectroscopy could be used as clinical tool to identify the chemical composition of calcified cornea and this information will help in the understanding of diseases related to the cornea.

Also, Raman spectroscopy has been used to investigate the aging of the lens and its related protein concentration with increasing age. Siebinga and colleagues (Siebinga et al., 1992) analysed the water and protein content in extracted human lenses using Confocal Raman spectroscopy. The findings of their study revealed the capability of using Raman spectroscopy to identify changes occurring in ocular tissues since they were able to find similarities between cortical proteins of 'old' and 'young' crystalline lenses. Furthermore, Duindam and colleagues (Duindam et al., 1998) analysed cholesterol, phospholipid, and protein in focal opacities in human donor lenses using Raman spectroscopy. Their findings and conclusion show the feasibility of using Raman spectroscopy to analyse proteins as well as other biological molecules in the human lens since they were able to find elevated levels of cholesterol in the lens.

Furthermore, another variant of Raman spectroscopy has been used to investigate the vitreous in proliferative diabetic retinopathy. Sebag and colleagues (Sebag et al., 1994) applied Raman spectroscopy on vitreous obtained during vitrectomy from patients with diabetic retinopathy and patients with retinal detachment. They were able to show that Raman spectroscopy can be used to identify differences in vitreous composition between patients having proliferative diabetic retinopathy and control subjects without diabetes and this could act as a clinical diagnostic tool in this regard.

Finally, Raman spectroscopy has been used in the in vitro evaluation of the retina. Gellermann and Bernstein (Gellermann & P. S. Bernstein, 2004) used Raman spectroscopy to analyse excised postmortem retina from donors aged 7 to 60 years with no known history of ocular pathology and found that Raman spectroscopy could be used to identify changes in the structure of pigments lutein and zeaxanthin. Since these pigments are involved in the pathology of aged related macular degeneration, this study shows the feasibility of using Raman spectroscopy as a technique in understanding the development of the disease. Also, Evans and colleagues (Evans et al., 2009)

showed that future application of Raman spectroscopy on the biochemical content of the retina may become possible by means of technology for optical coherence tomography (OCT). They used Confocal Raman spectroscopy to analyse human and fresh porcine retina samples. They were able to map OCT data and biochemical Raman spectral maps simultaneously showing the possibility of using the two devices simultaneously as a diagnostic technique for diseases related to the retina.

From the above studies, it is evident that Raman spectroscopy has a huge potential for in vivo analyses of human ocular tissues. The successful application of Raman spectroscopy in ocular media in front and behind the aqueous humor as well as in analysing aqueous humor biomolecules like glucose indicates that it is feasible to apply this technique in the analysis of aqueous humor proteins. However, to attain such goals, there is the need for an instrument operating based on Raman principle that will be compatible for non-invasive clinical use to examine ocular tissues. This instrument should be simple and easy to use and must be safe for both the human subject and clinician. With the ability to non-invasively study ocular tissues and quantitatively estimate the concentrations of biomolecules in these tissues using the Raman spectrometer, clinical diagnosis and management of ocular disorders will be facilitated. There is current strong interest in developing non-invasive technologies that would assist in understanding disease process, diagnosis and management. The next section discusses the invention of a patented instrumental setup for ocular purposes for which a prototype serves the focus of the presented study.

1.4 A novel patented instrumental setup for non-invasive measurement of biomarkers in the aqueous humor of the anterior chamber by means of Raman spectroscopy

This invention provides a setup for non-invasively determining a quantity of analytes in the aqueous humor of the anterior chamber of the eye using Raman spectroscopy. The instrumental setup has been developed by Martin Larsen Medical As, Kongsberg Norway and is registered with the Swedish Patent and Registration Office. Figure 6 gives an illustration of the patented instrumental setup and a basic description of how it operates to analyse analytes in the aqueous humor.

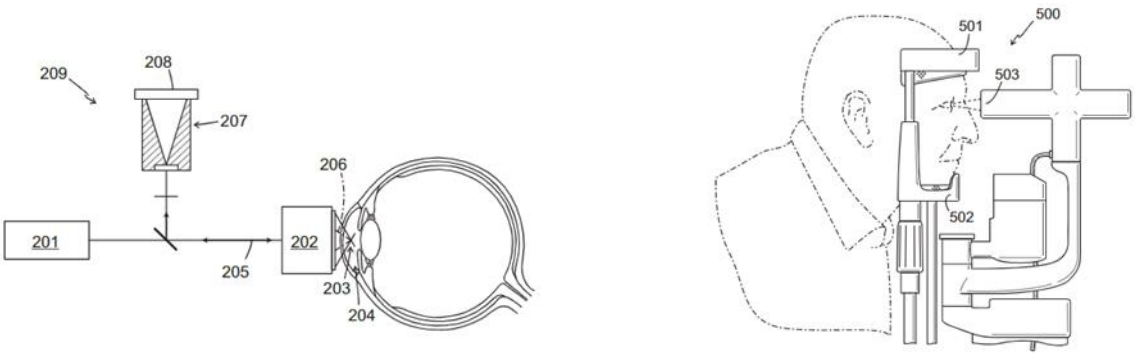

(a) (b)

Figure 6: Illustration of the patented instrumental setup showing (a) light scattering system and (b) side view of the setup with a headframe. The numbers in the diagrams represent the various parts of the setup and/or the process of operation. Courtesy: Martin Larsen (Inventor) with permission

The patented instrumental setup basically consists of a Raman spectrometer mounted on a slit lamp microscope to facilitate accurate analysis of aqueous humor in the anterior chamber (figure 6). In order to analyse an analyte in the aqueous humor (204) of the anterior chamber of the eye, an excitation of the sample is obtained by a light source (201). An optical probe (202) with focusing optics is used for directing and focusing the light toward a common focal sampling volume (203) of the anterior chamber of the eye. This results in the detection of at least a fraction of the inelastically scattered light (206) from the excited analytes in the sample volume (203) of the anterior chamber with a spectrometer (209) based on the Raman principle. The spectrometer (209) comprises a spectral disperser (207) and a detector array (208) that enable it to be used for measuring the spectral intensity distribution of Raman scattered light obtained from the sample (203). To enable in vivo real time measurements in a stable subject, the instrument provides a head frame (500) with forehead support (501) and chin support (502) for the person whose eye is the subject for measurement. To facilitate measurement of the anterior chamber when adjusting the position of the instrument, the instrument is attached to a slit lamp (503), such that the slit lamp and the optical probe are focused on a common point. Figure 7 gives an illustration of the pathway of laser input into the anterior chamber to analyse aqueous humor proteins and the pathway of spectral collection.

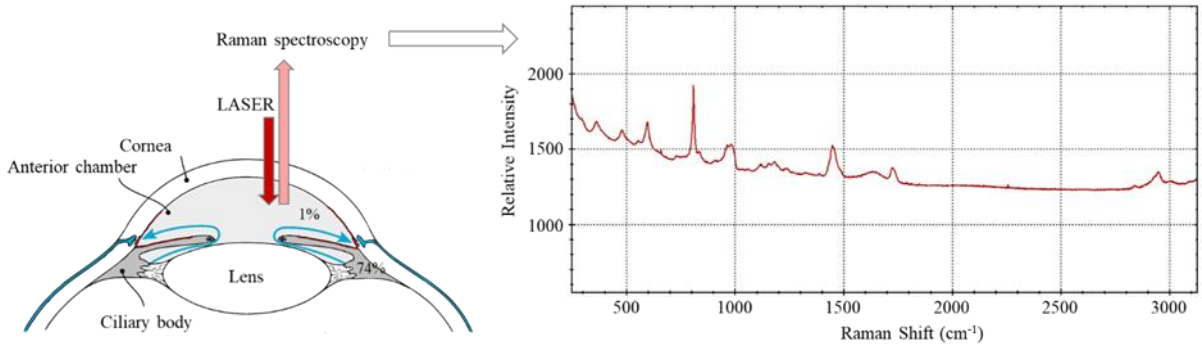

Figure 7: The anterior chamber of the eye (left picture). Blue arrows show the circulation of aqueous humor while red and pink arrows show measurements of protein composition in the chamber water by means of Raman spectroscopy. Results from Raman spectroscopy (right image) of a sample with low protein concentration. The bands in the spectrum provide a "fingerprint" of the protein composition. The height of the peaks reflects the concentration (from a pilot study at SINTEF, Oslo).

With focus of the device based on the analysis of the human aqueous humor (hAH), it is necessary to discuss the composition of the hAH in healthy eyes and eyes with disease. The aqueous humor is of more importance because many eye diseases are associated with changes in the composition of the hAH.

1.5 The human aqueous humor (hAH)

The human aqueous humor is the clear fluid filling the anterior segment (consisting of the anterior and posterior chambers of the human eye) between the corneal endothelium, the lens and the retrolental compartment (Bennett et al., 2010). It has an estimated volume of about 0.25 ml in the average adult (Rajagopalan, Advani, Pinto, & Goel, 2015) and performs several functions that include maintaining the intra ocular pressure, supplying nutrients to the avascular tissues of the eye, remove waste from the avascular tissues, antioxidation as well as immune response roles (Richardson et al., 2009). It is produced at an average rate of 2.0 – 2.5 µL/min (American Academy of Ophthalmolgy, 2020) from the non-pigmented ciliary body epithelium with an estimated turnover rate of 1.0 % to 1.5 % of the anterior chamber volume per minute (Kaufman & Alm, 2003). The hAH is composed primarily of water (99.9 %) and trace amounts of proteins, sugars, vitamins, and other nutrients as well as growth factors and cytokines (Tamhane, Cabrera-Ghayouri, Abelian, & Viswanath, 2019).

1.5.1 Aqueous humor proteins in the healthy eye

The human aqueous humor contains a minimal amount of proteins. Tight junctions of the non-pigmented ciliary epithelium and the iris vasculature endothelium are key elements of a blood-aqueous barrier that prevent plasma-derived proteins from entering the aqueous humor of the anterior and posterior chambers under normal conditions (Freddo, 2013).

Despite tight junctions of the blood-aqueous barrier, it has been estimated that aqueous humor proteins constitute about 1 % of plasma proteins. This paradoxical presence of plasma proteins in the aqueous humor is explained by a current model of the blood-aqueous barrier where plasma proteins diffuse from capillaries of ciliary body stroma, into the iris stroma and then to the anterior chamber (Freddo, 2013). Figure 8 is an illustration of the structure of the anterior segment of the eye showing the inflow of the estimated 1 % of plasma proteins into the anterior chamber.

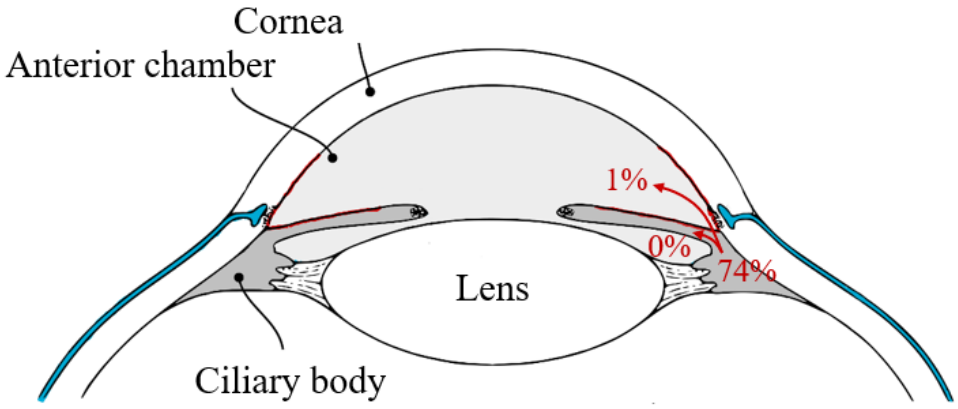

Figure 8: Illustration of the anterior segment of the eye showing the inflow channel of the estimated 1 % of plasma proteins into the anterior chamber depicted with the red arrow.

Freddo (Freddo, 2013) states that according to the current model of the blood-aqueous barrier and the inflow of plasma proteins into the hAH, the posterior chamber is essentially plasma-protein-free. Additionally, it has been observed that some of the protein delivered to the iris root

immediately enters the trabecular outflow pathways and does not stay in the aqueous humor. Furthermore, the entry of protein into the anterior chamber angle, by-passing the posterior chamber described in the current model is consistent with previous models of AH production that suggest AH as it is secreted is a plasma protein-free fluid. This however excludes proteins like transferrin that reach higher concentrations in aqueous than in plasma due to active transport (Freddo, 2013).

Proteomic studies of the proteins in the hAH are limited by a number of factors which include interfering high abundance proteins, inadequate animal models, and limited proteomic technologies (Richardson et al., 2009). Table 2 illustrates a summary of some important studies done on aqueous proteins and their concentrations.

Study	In vitro/In vitro: Medium	Method	Concentration Range
(Sen, Sarin, & Saha, 1977)	In vitro: 44 senile cataract patients undergoing cataract extraction	Standard Immunodiffusion	IgG: 0.015-0.176 mg/ml
(Mathis, Malecaze, Bessieres, Arne, & Seguela, 1988)	In vitro: 14 subjects undergoing routine cataract extraction or retinal detachment surgery	Immunonephelometry	Albumin: 0.21-0.62 mg/ml IgG: 0.015-0.12 mg/ml
(Ghose, Qiugley, Landrigan, & Asif, 1973)	5 Senile cataract patients undergoing cataract extraction	Radial immunodiffusion	IgG: 0.05-0.085 mg/ml
(Murray, Hoekzema, Luyendi, Konings, & Kijlsrra, 1990)	In vitro: 18 Senile cataract patients undergoing cataract extraction	Enzyme-Linked Immunosorbent Assay, Isoelectric Focusing, and Immunoblotting	Albumin: 0.02-2.08 mg/ml Average; 0.27 mg/ml

Table 2: Summary of some important studies done on aqueous proteins showing method of analysis and concentrations determined

The proteins Albumin and Immunoglobulin G (IgG) are among the major aqueous humor proteins with various studies giving slightly varying concentrations. Sen and colleagues (Sen, Sarin, & Saha, 1977) using the Standard immunodiffusion method of protein analysis reported an average

concentration of IgG; 0.07 ± 0.04 mg/ml . This was an in vitro study using aqueous humor obtained from patients who underwent cataract extraction. Mathis and colleagues (Mathis et al., 1988) reported measurement of Albumin and IgG concentrations of about 0.21 - 0.62 mg/ml and 0.015 - 0.12 mg/ml respectively. They obtained this by doing Immunonephelometry on aqueous humor derived from 14 subjects who underwent routine cataract extraction or retinal detachment surgery. Ghose and colleagues (Ghose et al., 1973) used Radial immunodiffusion to analyse the aqueous humor obtained from senile cataract patients and found the concentration of IgG as: 0.05 - 0.085 mg/ml. Murray and colleagues (Murray et al., 1990) used the ELISA method to do an in vitro aqueous humor analysis of 18 senile cataract patients who underwent cataract extraction and they detected an Albumin concentration range of 0.02 - 2.08 mg/ml with an average IgG concentration of 0.03 mg/ml.

Even though these studies are not very recent, they appear to be most significant in meeting the theme of our study. These studies reveal that Albumin is the most abundant protein in the human aqueous humor and because of difficulties in obtaining aqueous humor from subjects who are not undergoing ocular surgery, the cataract patients who have no history of ocular inflammation/disease represent physiologic cases. The study by Murray and colleagues (Murray et al., 1990) give a plausible physiologic concentration range of Albumin which is the main protein under investigation in this study as 0.02 - 2.08 mg/ml. For IgG, the study by Sen and colleagues (Sen et al., 1977) give a plausible IgG concentration range of 0.015 - 0.176 mg/ml. These findings give us an understanding of the physiologic concentration range of the protein Albumin in the healthy human aqueous humor and this formed the basis for the preparation of the samples for this present study.

1.6 Aqueous humor proteins as biomarkers of disease

Biological markers (biomarkers) have been defined by Hulka (Hulka, 1990) as cellular, biochemical or molecular alterations that are measurable in biological media such as human tissues, cells, or fluids.

Proteins in the hAH are thought to be involved in development of several eye diseases (Klenkler & Sheardown, 2004). Thus investigating the AH proteome will facilitate understanding regarding the

etiology of such pathologies (Richardson et al., 2009). Most studies conducted in this regard focused more on the characteristics of the proteins in ocular disease rather than quantifying them like the studies mentioned in table 2.

Izzotti and colleagues (Izzotti, Longobardi, Cartiglia, & Saccà, 2010) explored aqueous humor protein content from primary open angle glaucoma (POAG) patients (cases) and senile cataract patients (controls) by in vitro analysis. They found that a proteome content was significantly modified in glaucoma cases as opposed to controls and this was highly predictive for disease status of POAG. Xiang and colleagues (Xiang et al., 2017) investigated proteins in the aqueous humor in patients undergoing cataract extraction with no other ocular disease in an in vitro setting using iTRAQ labeling and Liquid Chromatography - Mass Spectrometry (LC - MS). They were able to identify 44 proteins in the AH associated with cataract formation. Duan and colleagues (Duan et al., 2008) sampled AH from patients with myopia and control cataract patients without myopia. They did in vitro protein analysis using mass spectrometry on the samples and found out that the total protein concentration in AH with high myopia was significantly greater than that of non-myopia indicating that AH proteins can act as biomarkers for myopia. Ghose and colleagues (Ghose et al., 1973) applied radial immunodiffusion to estimate quantitatively IgG, IgM, and IgA in the aqueous humor obtained before surgery from patients suffering from active chronic endogenous uveitis, narrow angle glaucoma with no active inflammation and senile cataracts. They found that all the patients with active uveitis showed elevated levels of immunoglobulins in the aqueous humor compared with subjects having glaucoma and senile cataract. This shows that increased levels of proteins in the aqueous humor may be used as biomarkers for the diagnosis of uveitis.

The above studies show that proteins can be important biomarkers for several eye diseases and hence the importance of the developed patented instrumental setup. Thus, with the above background and the preceding literature which highlight the importance of analysing the AH proteins, this study marks the first phase of a series of studies aimed at providing eye care professionals a novel non-invasive instrumental setup that can provide qualitative and quantitative analyses of AH proteins of patients for diagnostic purposes, management and monitoring.

2 Aims and objectives

The main objective of the study was to perform an initial in vitro validation of a novel system for non-invasive measurements of proteins in the aqueous humor of the anterior chamber of the eye by means of an adapted Raman spectrometer mounted to a commercial slit lamp microscope. The main objective was based on the following research questions related to the characteristics of the spectrometer measurements:

1. What is a feasible trade-off between averaging of measurements and number of samples to obtain a noise cancelling effect on the Raman shift intensity?
2. What is the repeatability of measurements of Albumin within a physiologic range of concentrations?
3. Is it possible to measure concentrations of Albumin within a physiologic range of concentrations?
4. Are measurements of physiologic concentrations of Albumin linear?

2.1 Significance of the study

Results are expected to provide important evidence for measurement principles of a patented instrumental setup of Raman spectroscopy in hAH. This includes an understanding of the stability of measurements of low concentrations of a protein and whether or not it is possible to obtain reliable measurement of a protein in its physiologic range. Results will also provide information about the extent to which measurements predict protein concentrations within a physiologic range.

3 Methods

3.1 Study design

The study had an experimental in vitro design and was conducted in the Goldmann Research laboratory of the National Center for Optics, Vision and Eye Research at the University of South-Eastern Norway, Norway.

The major components of the experimental setup (figure 9) consisted of a model eye and holder, a slit lamp microscope, and a commercial Raman spectrometer modified with a collimator lens. The instrumental setup is based on the description in section 1.4 of Chapter 1. The system was connected to a computer to enable acquisition of the spectral data for analyses. Bovine Serum Albumin was used as sample for the study and all the measurements were made by the same observer Issah Imoro (I.I).

(a) 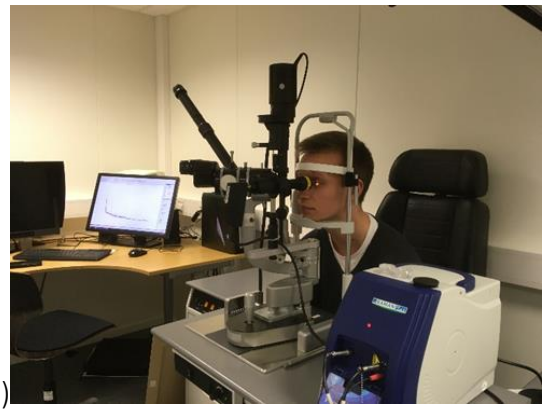 (b) 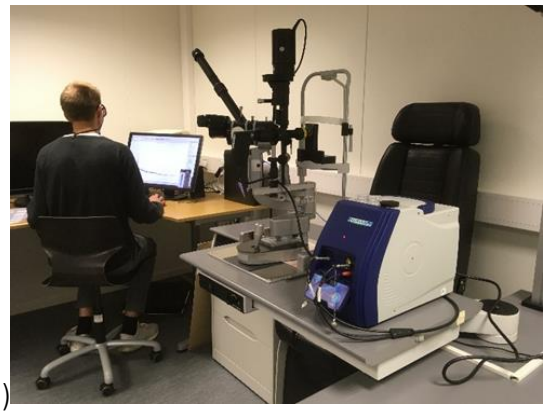

Figure 9: Images of the experimental setup showing (a) a patient positioned in the headrest to demonstrate intended use and (b) the experimental setup with the patient replaced with a model eye: By permission of the inventor Martin Larsen (pictured).

3.2 Instrumentation

3.2.1 Raman spectrometer

Previously we discussed in detail the patented instrumental setup invented for the study in Section 1.4 of Chapter 1. The following section augments that information and provides some detail on the specifications of the Raman spectrometer. The spectrometer that was used in the instrumental setup was an i-Raman Plus (BWTEK Model BWS465-785S, BW-TEC AG, Germany) for conventional Raman spectroscopy (figure 10). The spectrometer has a diode laser of 785 nm with 30 mW output power connected via fiber optics to a probe (RTS200-VIS-NIR, BW-TEC AG, Germany) and a confocal 15 µm aperture pinhole. We used light of wavelength 785 nm which falls within the Near Infrared range and has been shown to have minimal absorption by the cornea and lens with no record of accumulated damage from photochemical toxicity (Mellerio, 1994). The light within this wavelength optimizes transmission to and from the aqueous humor and minimizes the risk of damage to the tissues closest to the focal plane (Pelletier et al., 2005). Scattered light was detected by a back illuminated deep depletion Pelletier cooled (-70 °C) Charge Couple Detector (CCD). The CCD is of high quantum efficiency with deeper cooling and high dynamic range which makes it possible to measure weak Raman signals. The spectrometer provides 4.5 cm^{-1} resolution with a 50000 ms acquisition time in the 3000 - 200 cm^{-1} spectral range.

Figure 10: Image of i-Raman Plus (BWTEK Model BWS465-785S, BW-TEC AG, Germany) used for this study

3.2.2 Collimator lens

The model of the collimator lens is the RTS Series Raman zoom lenses, BW-TEC AG, Germany designed to work for Raman applications requiring longer working distance like this study. The laser light is focused through the front tube. The collimator lens was used to convert divergent light beams entering the spectrometer into parallel beams to enhance collection efficiency and spatial resolution of the sampling.

3.2.3 Slit lamp microscope

The collimator lens was mounted in the pivot hole of a standard slit lamp (Haag-Streit BQ 900) shown in figure 9 having 40X instrument magnification. Light source was a 27 W halogen bulb. The extra weight on the slit lamp was counteracted by springs mounted under the microscope tower.

3.2.4 Model eye and holder

Figure 11 is an image of the model eye and holder. The model eye was designed in the form of a small plastic container having a volume of 4 ml with a round hemispherical window representing the cornea. The hemispherical window consisted of a thin plastic scleral lens with a diameter of 14.00 mm, a Back-Optic Zone Radius (BOZR) of 8.04 mm and a Back-Vertex Power (BVP) of -3.00 D. The scleral lens was glued to the plastic container with Dibutylphthalate Polystyrene Xylene (DPX) and decentered by 4 mm to allow samples of 3 ml to cover the diameter of the lens. The model eye holder was a plastic with a central groove in the shape and size of the model eye. It was aligned in a central position and attached inferiorly to the chin rest and superiorly to the headrest of the slit lamp. The holder has a thin plastic sheet screwed superiorly to hold the model eye firmly in place to avoid it from falling off during measurements.

(a)  (b) 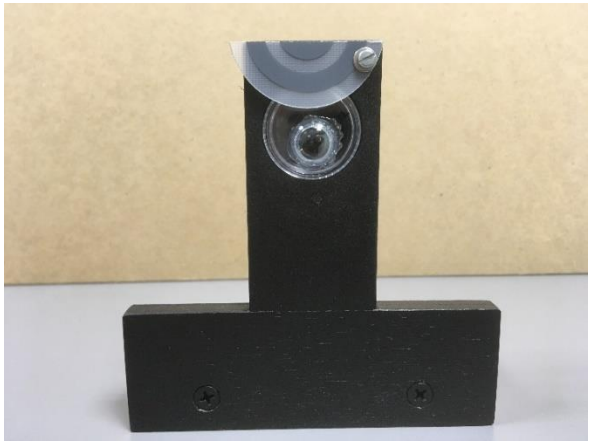

Figure 11: Image of (a) the model eye alone and (b) the model eye firmly fixed in the holder

3.3 Study sample

The study sample consisted of 16 samples each 3 ml of solutions of Bovine Serum Albumin (BSA) of concentration range 0.2 - 3.0 mg/ml (table 3). The 16 samples were either assigned as low, medium or high-level concentration and were used for 3 different kinds of measurements namely concentration, repeatability and standard deviation presented in table 3.

Sample	Concentration mg/ml / (%)	Measurement type and number	Concentration level	Error (mg/ml)
A1	0.0 (0.00)	Standard deviation; 25 times	Low	0.00
A2	0.2 (0.02)	Concentration	Low	0.20 ± 0.03
A3	0.4 (0.04)	Concentration	Low	0.40 ± 0.05
A4	0.6 (0.06)	Concentration	Low	0.50 ± 0.08
A5	0.8 (0.08)	Concentration	Low	0.80 ± 0.10
A6	1.0 (0.10)	Concentration	Low	1.00 ± 0.13
A7	1.2 (0.12)	Concentration	Medium	1.20 ± 0.15
A6	1.4 (0.14)	Concentration	Medium	1.40 ± 0.18
A9	1.6 (0.16)	Concentration	Medium	1.60 ± 0.20
A10	1.8 (0.18)	Concentration and Standard deviation; 25 times	Medium	1.80 ± 0.23
A11	2.0 (0.20)	Concentration and Repeatability; 5 times	Medium	2.00 ± 0.26
A12	2.2 (0.22)	Concentration	High	2.20 ± 0.29
A13	2.4 (0.24)	Concentration	High	2.40 ± 0.31
A14	2.6 (0.26)	Concentration	High	2.60 ± 0.34
A15	2.8 (0.28)	Concentration	High	2.80 ± 0.26
A16	3.0 (0.30)	Concentration	High	3.00 ± 0.39

Table 3: Samples with associated measurement type, concentration level and error in concentration due to mixing protocol. Concentration is presented in mg/ml and percent.

Table 4 illustrates the mixing protocol used to obtain the samples. The test samples were prepared from 5% BSA in 0.85% sodium chloride (Merck Life Science AS, 2020) and diluted with 0.85 % saline to obtain concentrations as shown in table 3. Dispensing of volumes was manual pipetting using reference pipettes of 1-10 ml (Batch J436023G) and 100-1000 µl (Batch I435462P) (Eppendorf Reference® 2G, Eppendorf, Germany figure 12a) according to the protocol in the table 4. Samples were mixed in clean vials and then stored in a refrigerator at a temperature of +4.00 degrees celsius before analysis (figure 12b).

Vial	Albumin (µl)		Saline (µl)		
A1	0	120	1000	1000	1000
A2	0	240	960	960	960
A3	0	360	920	920	920
A4	0	480	880	880	880
A5	0	600	840	840	840
A6	0	720	800	800	800
A7	0	840	760	760	760
A8	0	960	720	720	720
A9	0	540	680	680	680
A10	540	120	0	960	960
A11	600	600	0	900	900
A12	660	660	0	840	840
A13	720	720	O	780	780
A14	780	780	0	720	720
A15	840	840	0	660	660
A16	900	900	0	600	600

Table 4: Protocol for mixing Albumin and saline to obtain samples for the measurements. Each column is a pipetting load. (i.e. maximum two loads of Albumin and three loads of saline).

(a) 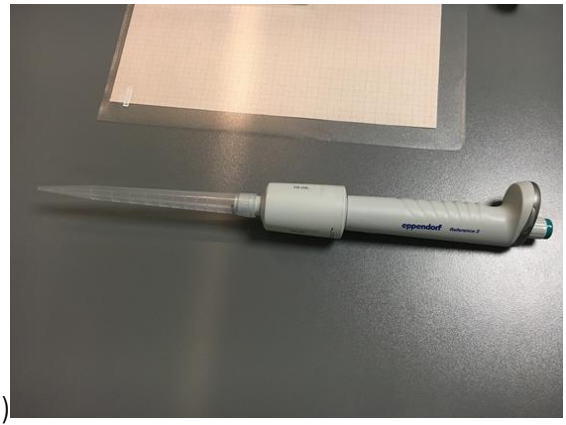 (b) 

Figure 12: Image of (a) Eppendorf 1-10 ml pipette used for preparing the test samples stored in (b) clean vials and held on a wooden rack for storage in the refrigerator

3.4 Protocol

3.4.1 Pre-measurement adjustments

Pre-measurement adjustments included proper focusing of the eye pieces at 40X magnification, focusing and alignment of the collimator lens. The purpose of focusing eye pieces was to achieve alignment of the microscope and illumination system of the slit lamp. Magnification was the same as the magnification used in the measurement protocol. To achieve accurate focusing we used the focusing rod placed in the pivot hole of the slit lamp and a medium width beam (figure 13). The eyepieces were then rotated fully anti-clockwise, producing maximum plus, before each eyepiece was focused individually by rotating the eyepiece clockwise, decreasing the plus, until the appearance of the slit beam on the focusing rod was clear. After reaching the endpoint care was taken not to rotate the eyepiece further to avoid inducing accommodation in the examiner (I. I). We then separated the eyepieces to a comfortable pupillary distance of 64 mm for the observer so as to allow a comfortable and clear binocular view of the focusing rod surface.

Figure 13: Adjustment of light using the focusing rod in the pivot hole of the slit lamp

In order to obtain spectroscopic sampling from a point that corresponded with the axial and lateral position of the light slit, the focusing rod was removed and the microscope was rotated about 45 degrees from the primary position while the light tower remained in primary position. The light slit was thereafter placed in focus on the surface of a thin plastic sheet mounted on a separate model eye for focusing purposes (figure 14) and the slit lamp was locked in this position.

Figure 14: Light slit placed in focus on the surface of a thin plastic sheet mounted on a separate model eye for focusing

The light tower was rotated in front of the microscope (45 degrees from primary position) and the collimator lens was swung to the primary position. Proper axial adjustment of the collimator lens was obtained by identifying the position that gave the strongest signal in a series of continuous spectroscopic measurements from the plastic sheet. In order to find proper lateral adjustments, the model eye was replaced with a model eye having a 1 mm wide plastic strip (figure 15). Keeping the focusing distance unaltered the lateral position was adjusted in the horizontal direction (strip in vertical direction) and thereafter in the vertical direction (strip in horizontal direction) using the same methods as for axial adjustments.

Figure 15: Model eye with a 1 mm wide plastic strip used for lateral adjustments of the light slit

3.4.2 Measurements

The samples were tested in an increasing numerical order of labelling from A1 to A16 (table 3). The vial containing a test sample was opened and the content transferred into the model eye. The model eye was then placed firmly in position in the holder (figure 11b) and the slit lamp was powered. The collimator lens was swung to one side and the light tower was rotated to primary position while the microscope was at approximately 45 degrees from primary position. The light was then focused on the surface of the scleral lens of the model eye representing the cornea. In order to obtain measurements from the assumed anterior chamber of the model eye, the slit lamp was moved 2 mm from the point of focus in axial direction towards the model eye using graph paper with a millimeter grid as reference (figure 16). The slit lamp was thereafter locked in this position.

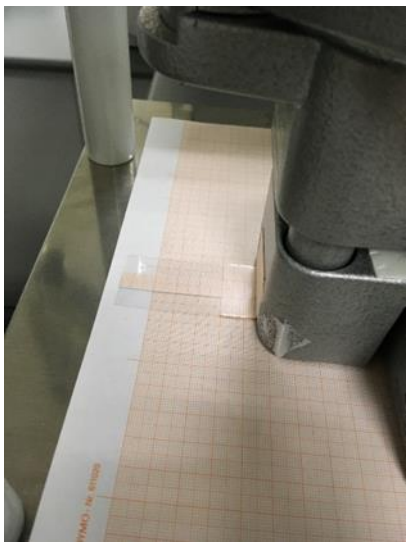

Figure 16: An image showing the graph attached to the slit lamp to enable 2 mm movement towards the model eye

The illumination system of the slit lamp was rotated 45 degrees to a position in front of the microscope, and the probe of the Raman spectrometer positioned in primary position in line with the model eye (figure 17). Measurement was done in dim light to reduce photoluminescence.

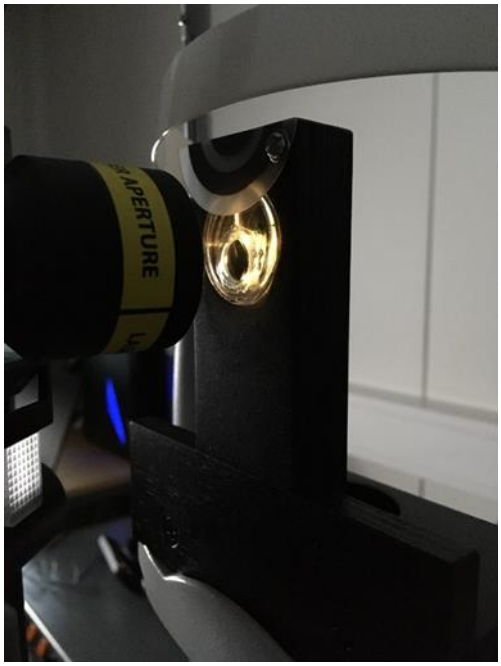

Figure 17: Probe moved 2 mm toward the model eye and aligned for measurement

The spectrometer was then powered on, and the acquisition time set to 50000 ms with averaging set to 12 samples on the computer and then measurements were done with spectra collected at 30 mW output power.

One model eye was used for all test samples and so after the measurement of each sample the Albumin solution was discarded in a drain and the model eye washed thoroughly using saline and wiped clean using a clean tissue before introducing the next test sample.

Spectral data for each measurement was saved in the American Standard Code for Information Interchange (ASCII) format directly on the computer connected to the experimental setup using the BWIQ V.2.1.1 software.

3.5 Analyses

Chemometric analyses were performed with the Unscrambler X version 10.5 (CAMO Software AS, Oslo, Norway) which is a leading software in spectral data analyses. The software was used to import the data for visualization, signal processing and multivariate statistical analyses.

3.5.1 Analyses related to a feasible trade-off between averaging of measurements and number of samples to obtain a noise cancelling effect on the Raman shift intensity

Simulation was performed to investigate the effect of averaging of repeated measurements on the estimated variance of the mean of the saline (i.e. 0.0 mg/ml) sample. The reasoning was that randomized noise will cancel itself out whereas the true signal will remain unaffected when averaging repeated measurements. Simulation was based on a Gaussian distribution with mean equal to zero and modifiable spread given as standard deviation (SD). Each simulation provided estimated mean, averaged from 2 – 25 repeated measurements in sequence. We performed 100 simulations on 2 – 25 repeated measurements in order to determine the 95 % confidence interval (CI) for the estimated mean. Target was chosen as the number of repeated measurements (samples) when the CI of the estimated mean is close to half the SD of the variability of the

underlying Gaussian distribution. Simulation was performed for Gaussian distributions with averaged standard deviation for the fingerprint region (1700 - 500 cm^{-1}) calculated by averaging the spectral intensities for this region. This region was chosen because it contained spectral band 1650 cm^{-1} which was the band of interest in this study and was the most prominent band corresponding to Amide I unique to proteins. The results obtained from the simulation formed the basis for choosing to sample 12 times for each acquisition.

3.5.2 Analyses related to the repeatability of measurements of Albumin concentrations

This was done by using the statistics of the preprocessed data of the 5 repeatability measurements to calculate the coefficient of variation (cv). The standard deviation and mean relating to the band 1650 cm^{-1} of the preprocessed data of the repeatability measurements were used to calculate the coefficient of variation. Preprocessed data was chosen because it provides reduced effects of noise on the data statistics that was relied on for the calculation. CV was calculated as:

$$cv = \frac{standard\ deviation}{mean} \qquad (1.3)$$

3.5.3 Analyses related to whether it is possible to measure concentrations of Albumin within a physiologic range of concentrations

Data processing of the Raman spectra was carried out in the fingerprint region (1700 - 500 cm-1). A smoothing Savitsky-Golay of a Polynomial order 2 and 3 smoothing points was applied to smoothen the spectra followed by a standard normal variate (SNV) transformation for baseline correction and normalization. Preprocessing included exclusion of artefactual responses shown as negative spikes.

Principal component analysis (PCA) with full cross validation using 16 segments excluding outliers was employed to visualize the underlying information from the multivariate fingerprint spectral dataset of the 16 samples of BSA to reveal whether physiologic low concentrations could be measured. We used the scores plot to look out for clusters, outliers and significant patterns

associated with the data points (samples) and whether there is any interaction between the data points.

3.5.4 Analyses related to whether measurements of physiologic concentrations of Albumin are linear

PLS was run on the data to establish the predictive ability of the model using the predicted vs reference of both calibration and validation plots to show linearity of the measurements. We used the slope of the calibration and validation pls regression line to determine the linearity of the measurements. The R2 of the PLS regression fit also gave us information about the prediction ability of the model.

3.5.5 Analyses related to error analyses of Albumin concentration resulting from the mixing protocol

The systematic errors used for the error analysis were 0.13 % and 0.10 % for the Eppendorf pipettes 1-10 ml and 100-1000 µl respectively. Because sample concentrations were based on mixtures (table 4) error propagation for fractional uncertainties was used to estimate concentration errors for the samples. Estimated fractional errors were converted to mg/ml and are presented in table 3. The associated errors were determined by multiplying the corresponding systematic error value of the pipette used (with respect to the volume) to the expected concentration.

4 Results

In total, there were 46 measurements obtained: 25 related to research question 1 (feasible trade-off between averaging of measurements and number of samples to obtain a noise cancelling effect on the Raman shift intensity), 5 related to research question 2 (repeatability of measurements of Albumin within a physiologic range of concentrations), 16 related to research question 3 and 4 together (Is it possible to measure concentrations of Albumin within a physiologic range of concentrations; Are measurements of physiologic concentrations of Albumin linear respectively). Results are presented in the corresponding order below:

4.1 Results related to the investigation of a feasible trade-off between averaging of measurements and number of samples to obtain a noise cancelling effect on the Raman shift intensity

Simulations were based on the variability of 25 repeated measurements obtained from saline (i.e. 0.0 mg/ml concentration). The averaged SD for the fingerprint region (1700 – 500 cm^{-1}) was determined as 28.20 and this is depicted by the horizontal blue line in figure 18 which shows the results of the simulation. From the simulation, we found that the SD at 12 samples was close to half of the averaged standard deviation for the fingerprint region and this is shown by the intersection between the orange vertical line passing through the data point for 12 samples and the horizontal green line passing close to SD of 15 on the y-axis. This finding shows that 12 samples or more provides an estimated mean of the true signal with a 95% CI that is close to 0.5 SD of the variability of the true signal.

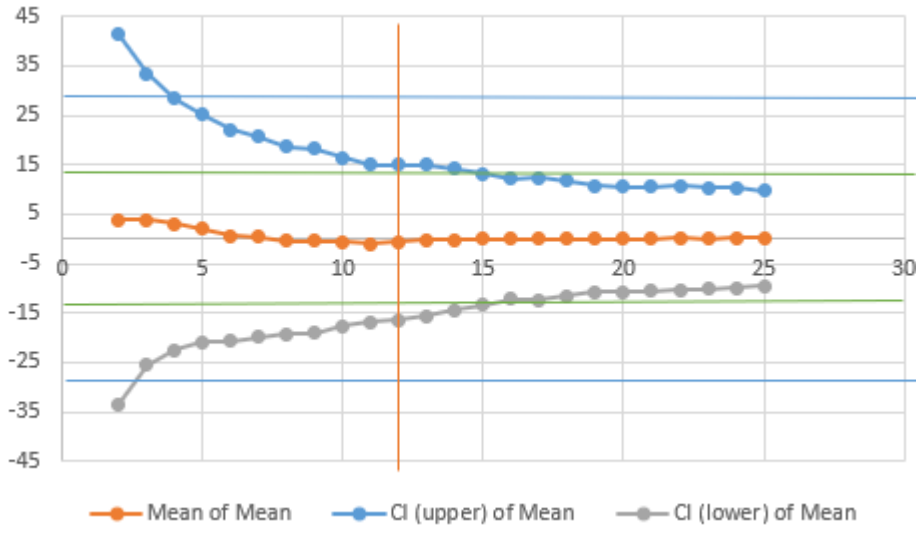

Figure 18: Results from simulation of measurements from saline 0.0 mg/ml showing noise is cancelled at 12 samples or more. x-axis represents number of samples and y-axis represents SD for mean of 100 simulations of 2-25 repeated samples. Graph also shows SD of 12 samples is approximately half of the averaged SD for the fingerprint region.

4.2 Results related to investigation of the repeatability of measurements of Albumin within a physiologic range of concentration

Preprocessed data that formed the basis for the investigation of the repeatability is displayed in figure 19 and table 5 shows statistics (preprocessed) obtained from the relevant band 1650 cm^{-1} that was used to calculate the coefficient of variation as 0.69 %.

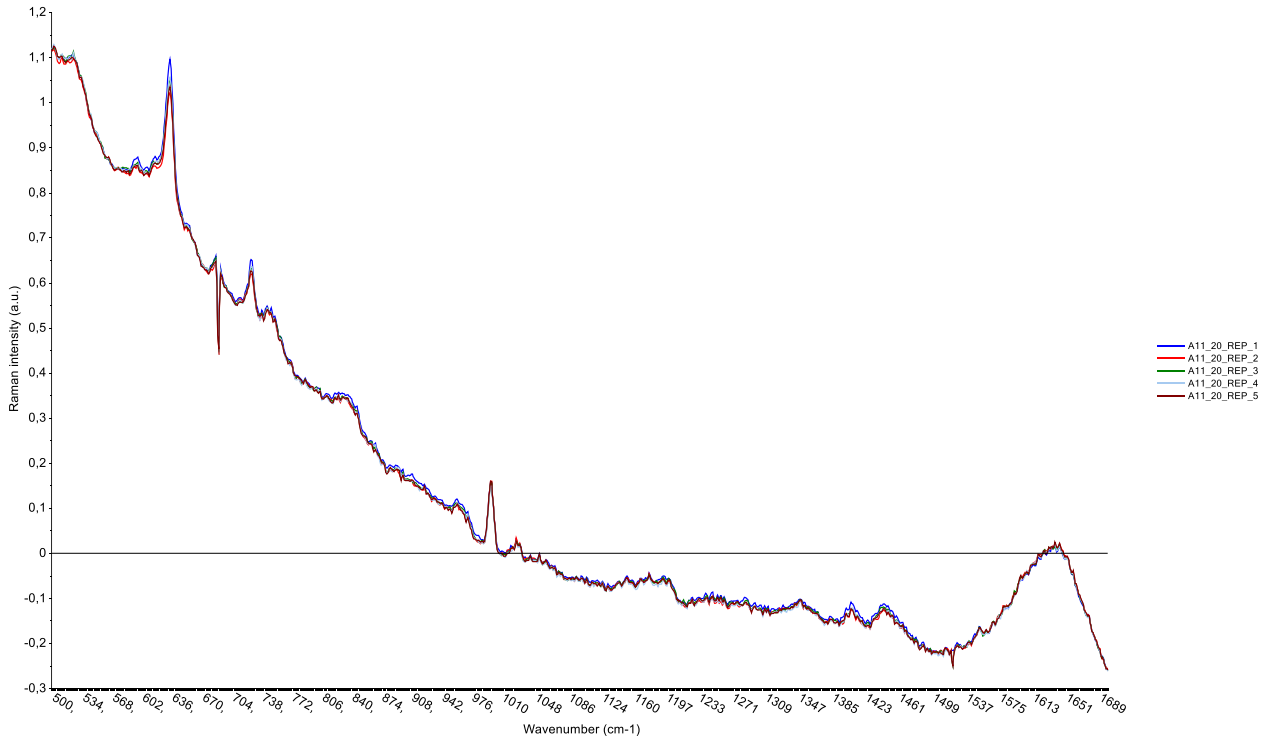

Figure 19: Line Plot of fingerprint region of Repeatability results after pre-processing using Savitsky-Golay with SNV showing a relevant peak at band 1650 cm^{-1} used for analyses of repeatability

Wavenumber (cm^{-1})	Mean	Maximum	Minimum	Std Deviation	Range	Variance
1650	4223.9540	4264.5280	4189.3490	29.2256	75.1787	854.1346

Table 5: Statistics (preprocessed) of chosen band 1650 cm^{-1} of Repeatability test showing standard deviation and mean used to calculate the coefficient of variance

Coefficient of variation was found to be 0.69 % for band 1650 cm^{-1}.

4.3 Results related to measurements of concentrations of Albumin within a physiologic range of concentrations

Preprocessed data for wavenumber range 1700 – 500 cm^{-1} is displayed in figure 20.

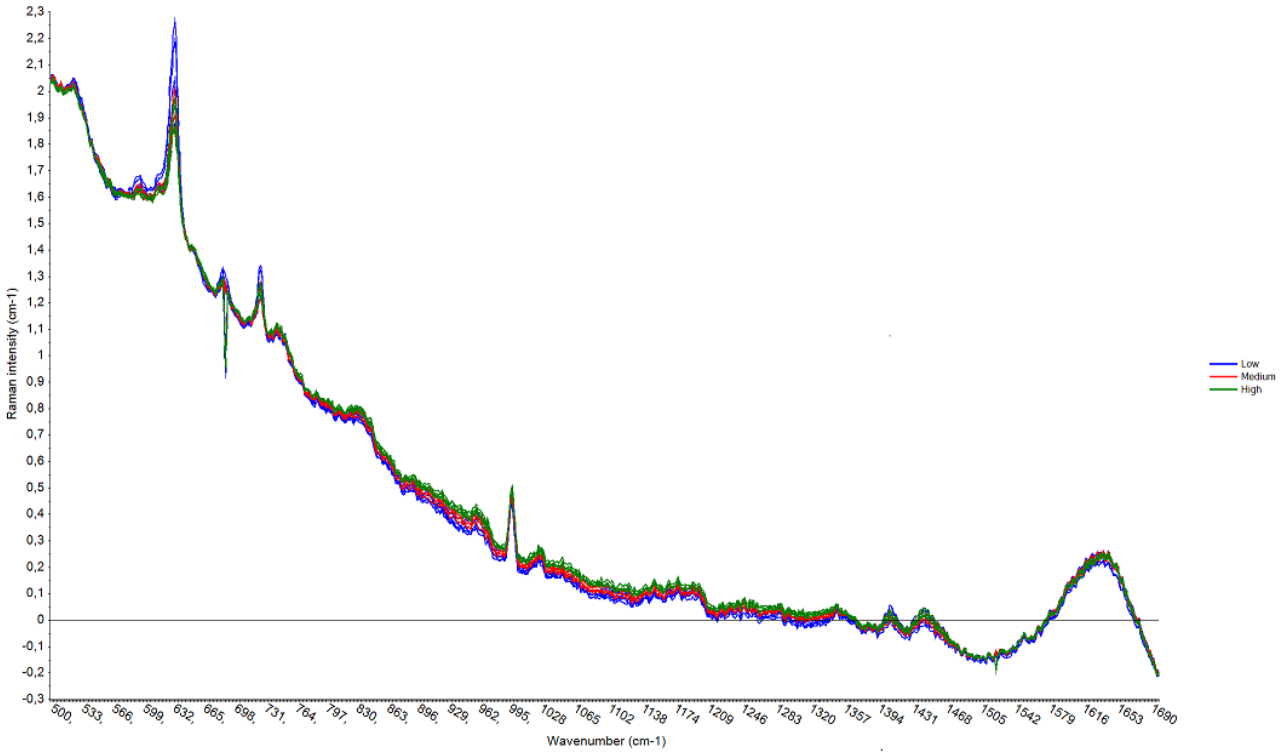

Figure 20: Line Plot- Fingerprint-Savitsky-Golay with SNV of concentration samples showing a peak at band 1650 cm^{-1}

Scores plot from the principal component analyses (PCA) is shown in figure 21. The results show grouping of samples based on concentration level indicating the ability of the model to quantitatively discriminate between low level concentrations (blue), medium level concentrations (red) and the high-level concentrations (green). PCA shows that the spread of the data points in the high-level concentration group was the lowest indicating a strong relationship between the samples in this group. Data points in the low-level concentration group had a larger spread indicating there is little interaction between those samples.

The results also show that there were no outliers since all the data points were within the Hoteling T^2 ellipse.

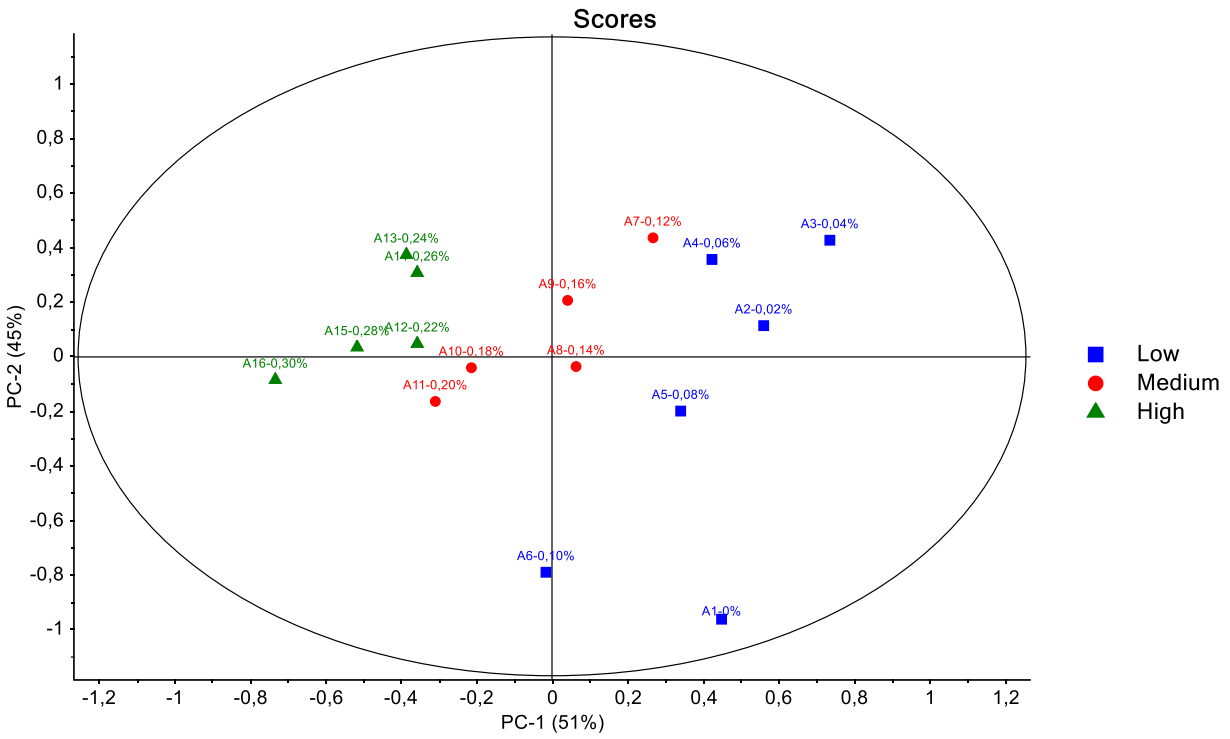

Figure 21: Scores plot from PCA with Hoteling T^2 ellipse showing the grouping of samples according to concentration level (quantitative discrimination). Concentrations of samples are given in percentage

4.4 Results related to the linearity of measurements of Albumin in the physiologic range

Results from the partial least square regression analysis are shown in figure 22. Results from the predicted vs reference plot for both calibration and validation models show there is good linearity (slope of 0.98) across the measurement. R2 values of 0.98 for both calibration and prediction indicate good prediction. Root mean square error cross validation (RMSECV) is 0.01 and this adds to the good prediction of the model.

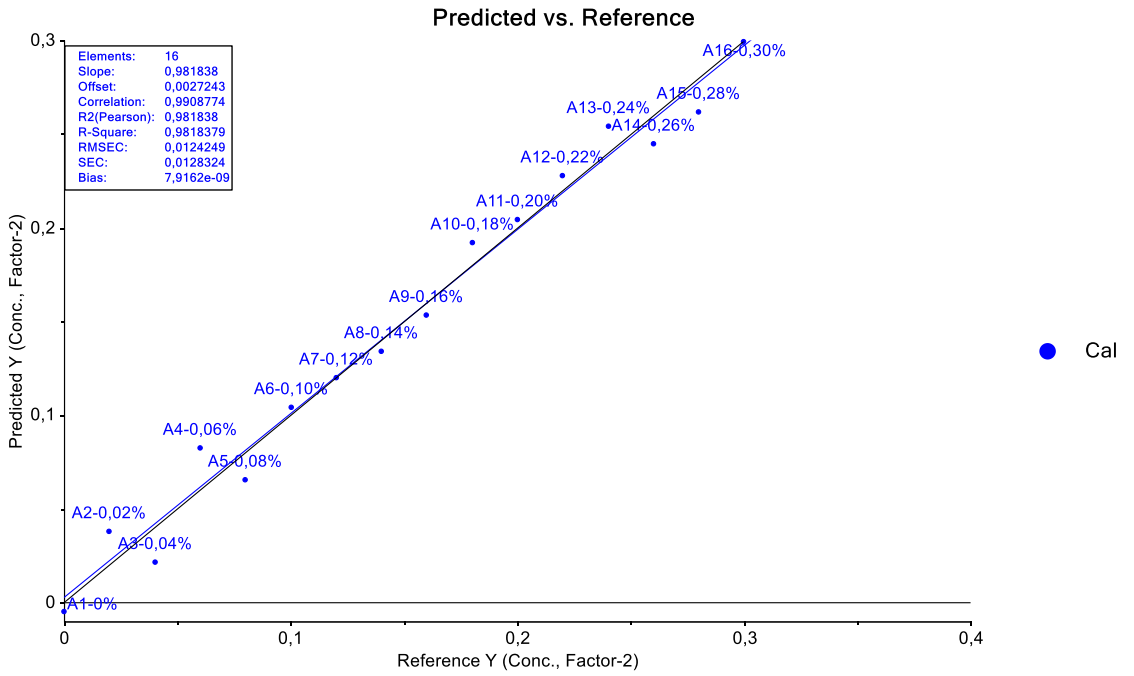

(a)

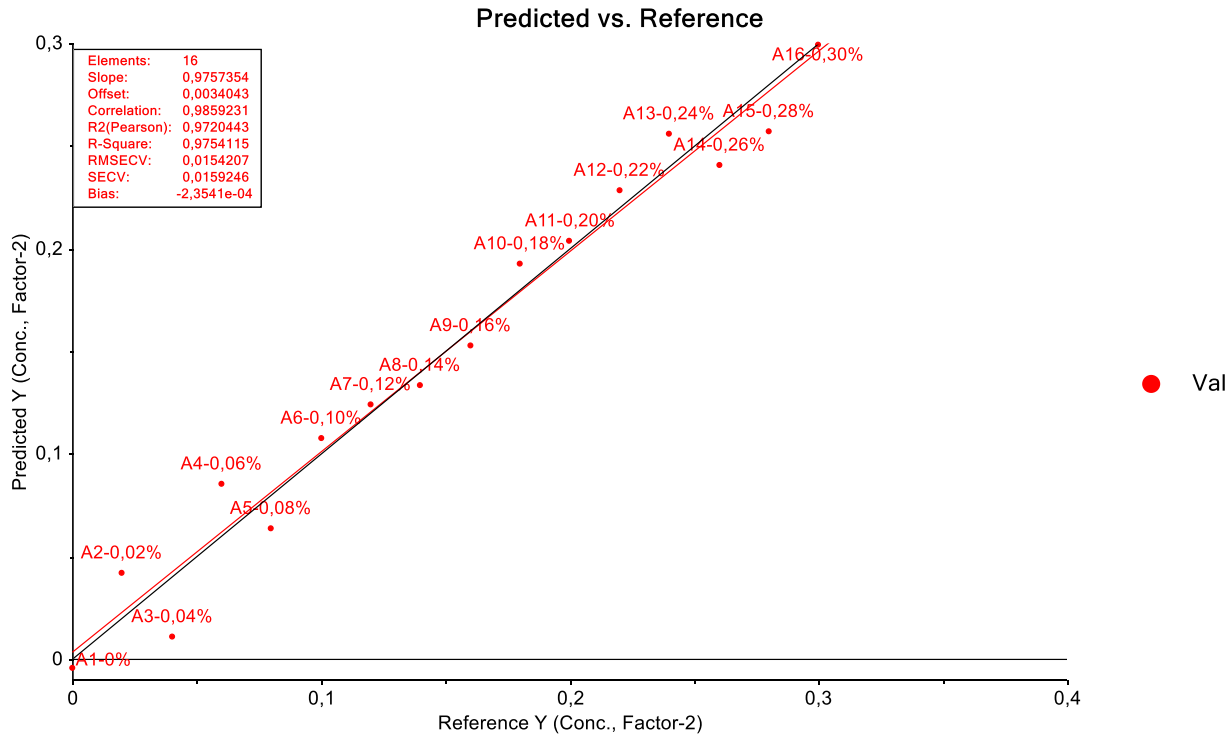

(b)

Figure 22: Predicted vs References plot of pls regression of (a) calibration model and (b) validation model showing good linearity of measurements with statistics inset. Concentrations of samples are given in percent

5 Discussion

In this present study, we investigated for first time the feasibility of a patented instrumental setup for non-invasive Raman spectroscopy of low concentrations of proteins in the aqueous humor using a model eye and Bovine Serum Albumin. We sought to first find out a feasible trade-off between averaging of measurements and number of samples to obtain a noise cancelling effect on the Raman shift intensity. Simulation indicated 12 samples for averaging as a feasible trade off. The repeatability of the measurements was determined to be 0.69 %. We also investigated whether it is possible to measure concentrations of Albumin within a physiologic range of concentrations and found support for achievable measurements down to 0.2 mg/ml based on chemometric analyses. Finally, we looked at the linearity of the measurements and found that the results showed a very good linearity.

5.1 Methodological considerations

A Raman spectrometer was the analytic tool of choice because it presents the advantage for non-invasive analysis of ocular tissues. In order to avoid the photoluminescence background often caused by biological samples, we chose excitation using near infrared (NIR) which is one of the major techniques to reduce photoluminescence (Zhao et al., 2010). We chose the Unscrambler software from Camo Analytics which is a well-established tool for chemometric analyses of spectroscopic data (Camo Analytics, 2020). Parachalil and colleagues (Parachalil, Brankin, McIntyre, & Byrne, 2018) state that preprocessing techniques are essential to remove the background signal and reduce the noise, before further analysis. Furthermore, we kept the preprocessing to a minimum in order not to lose information in contiguous Raman shifts (wavenumbers). This approach to preprocessing has been applied in studies to analyse human serum albumin (Artemyev et al., 2016).

Protein structure determines their functioning. We chose Albumin for the study because it is the most abundant protein found in human aqueous humor. However, our choice of Bovine serum Albumin (BSA) for the initial phase of this study was mainly because it is widely used as model globular protein for most studies (Abrosimova, Shulenina, & Paston, 2016) and because of its high stability, availability at high purity and its water solubility (Kopac & Bozgeyik, 2010).

5.2 A feasible trade-off between averaging of measurements and number of samples to obtain a noise cancelling effect on the Raman shift intensity

Because most analytical instruments produce a signal even when a blank sample (sample without analyte) is analysed (Wells, Prest, & Russ, 2011), our first question looked at what signal is a feasible trade-off between averaging of measurements and number of samples to obtain a noise cancelling effect on the Raman shift intensity. With the finding that averaging, and noise cancelling is obtained with 12 samples or more, it supports our choice to sample 12 times for each acquisition. By increasing the number of samples from 2 to 12 samples, standard deviation reduced from 28.20 to 15 (almost half of SD) depicting an approximate decrease in noise of about 50 %. With a confidence interval of 95 % it means measurements will provide an estimate of the true signal that is close to 0.5 standard deviation of the variability of the true signal 95 % of the times.

5.3 Repeatability of measurements of Albumin within a physiologic range of concentrations

Repeatability of a test describes the fraction of total variation in a set of measurements because of the variance among individuals and can be estimated using the coefficient of variation which is a normalized measure of dispersion of a probability distribution or frequency distribution. Hofko and colleagues (Hofko, Alavi, Grothe, Jones, & Harvey, 2017) suggest that the smaller the coefficient of variation (CV) is the smaller the scatter of results (in terms of standard deviation) relative to the mean value of a sample. Thus, our obtained CV of 0.69 % correlates with excellent repeatability of measurements for the 1650 cm^{-1} band. This is comparable to CV finding of 0.2 – 1 % range obtained by Gomez and colleagues (Gómez, Coello, & Maspoch, 2019) when they used Raman spectroscopy to investigate reproducibility of Raman spectra of compacted samples. This is also far better than the 20% maximum CV stipulated for many standardized laboratory measurements (Reed, Lynn, & Meade, 2002). This implies that measurements were very consistent with no significant variation and this means the results of the study are repeatable in measuring the concentrations of the Albumin in the physiologic concentration range studied.

5.4 Is it possible to measure concentrations of Albumin within a physiologic range of concentrations?

In this question, we sought to find out whether the patented instrumental setup had the ability to measure Albumin concentrations within the physiologic range i.e. 0.02 - 2.08 mg/ml. The test samples included concentrations between 0.2 mg/ml and 3.0 mg/ml. Using chemometrics, the ability of the scores plot from PCA analysis to discriminate, detect and group the low concentration level samples indicated that the patented instrumental setup had the ability to measure low concentrations of Albumin in physiologic range. Results of the PLS regression indicate that the patented instrumental setup was able to provide estimates (predict) concentrations of Albumin within a physiologic range down to 0.2 mg/ml since that was the minimum concentration level tested. However, the low concentration data points were distant from the regression line as compared to high concentrations and this suggests that predictions for low concentrations had a reduced certainty when compared to high concentration levels. Weak signals require chemometric analyses to subtract information related to photoluminescence. However, in this study we have for the first time demonstrated that Raman spectroscopy can be used to measure low concentrations of Albumin protein in a model eye. The errors in concentration of prepared samples associated with the mixing protocol may have had an impact in the true estimation of the model. This is particularly a problem since we did not verify concentrations of the prepared samples before the measurements. This could have been done using the ELISA method.

The Raman spectrum of the protein fractions is a set of bands corresponding to deformation and stretching vibrations of the carbon bonds with other elements (Artemyev et al., 2016). In our study, we used chemometrics to identify Albumin based on the peak observed at band 1650 cm^{-1} corresponding to Amide I. Artemyev and colleagues (Artemyev et al., 2016) in their analysis of human serum Albumin also found the maximal intensity in the Raman spectrum belong to the band 1650 cm^{-1}, corresponding to Amide I wavenumber. This result is critical to this study because it demonstrates the ability of the patented instrumental setup to not only quantify the analyte (Albumin) but also to identify its spectral characteristics.

5.5 Are measurements of physiologic concentrations of Albumin linear?

The results from the study indicated that the patented instrumental setup makes it possible to obtain linear measurements of low concentrations of Albumin in the physiologic range. The partial least square regression model showed good in prediction for the range of sample concentrations analysed with slope of 0.98 indicating good linearity. However, linearity was less obvious (greater uncertainty) for lower concentrations 0.0 – 0.8 mg/ml (from 0.0 % to 0.08 %) and improved with greater certainty for higher concentrations except for the 2.4 – 2.6 mg/ml (0.24 % – 0.26 %) range. Raman spectroscopy at low concentrations may be associated with several challenges mainly due to weak signals (Parachalil et al., 2018). This explains why the spread of the results in the low concentration group was greater than the high concentration group. This was despite the fact that we used excitation in the near infrared range that has been shown to reduce the effect of weak signals on the intensity. Future studies may explore the use of other variants of Raman spectroscopy like Coherent anti-stokes Raman spectroscopy that uses multiple frequencies to improve signal intensity for analysing tissues.

5.6 Limitations of the study and future direction

This study has a number of limitations. Major limitations were those relating to the Raman spectrometer such as the sensitivity of the photodetector and resolution of wavenumber which are usually due to the weak Raman signals. With the increasing interest for non-invasive technologies for medical purposes, Raman systems with higher sensitivities of photodetectors and strong resolution of wavelengths may be developed soon. An ambitious project of incorporating artificial intelligence to improve Raman sensitivity may be considered in future studies. Other limitations were associated with concentration errors resulting from the mixing protocol which were not verified after preparations and before the measurement. Acquisition was experimental with a laser effect that may need to be further modified for safe use in clinical setting. Because of the wavelength used which is longer than the shorter wavelength spectrum range, the total sampling time was also far beyond what is feasible in a clinical setting. Finally, photoluminescence which is a major limitation for most Raman spectrometers was reduced as much as possible using near infrared radiation since it has been proven to reduce the effect of photoluminescence in Raman studies.

Based on the results in the reported study, it is recommended to proceed with investigations of the sensitivity and specificity of the patented instrumental setup to complete the validation process. This should include the accuracy and precision assessment of verified concentrations of Albumin and other common proteins in the hAH like Immunoglobulin G.

6 Conclusion

The results of the reported study have for the first time shown that a novel patented instrumental setup for Raman spectroscopy of the molecular content of the aqueous humor is able to provide measurements of Albumin at physiologic concentrations down to 0.2 mg/ml with a high degree of linearity and repeatability from a model eye. Results provide important support for the principles of the patented instrumental setup and will form the basis for developing the patented instrument into a compatible device for in vivo clinical use for the diagnosis of ocular diseases.

References/bibliography

Aboul-Enein, H. Y., & Hoang, V. D. (2015). Raman Spectroscopy for Protein Analysis. *Applied Spectroscopy*.

Abrosimova, K. V., Shulenina, O. V., & Paston, S. V. (2016). FTIR study of secondary structure of bovine serum albumin and ovalbumin *Journal of Physics*. doi:10.1088/1742-6596/769/1/012016

American Academy of Ophthalmolgy. (2020). Aqueous Humor Formation. Retrieved from https://www.aao.org/bcscsnippetdetail.aspx?id=591e80ab-e372-4ad3-9c49-1aed4ba74f61

American Chemical Society. (1998). C.V. Raman and the Raman Effect. Retrieved from https://www.acs.org/content/acs/en/education/whatischemistry/landmarks/ramaneffect.html

Artemyev, D., Bratchenko, I., Khristoforova, Y., Lykina, A., Myakinin, O., Kuzmina, T., . . . Zakharov, V. (2016). *Blood proteins analysis by Raman spectroscopy method*.

Aslam, B., Basit, M., Nisar, M. A., Khurshid, M., & Rasool, M. H. (2017). Proteomics: Technologies and Their Applications. *Journal of Chromatographic Science, 55*(2), 182–196.

Bauer, N. J., Wicksted, J. P., Jongsma, F. H., March, W. F., Hendrikse, F., & Motamedi, M. (1998). Noninvasive assessment of the hydration gradient across the cornea using confocal Raman spectroscopy. *Invest Ophthalmol Vis Sci, 39*(5), 831-835.

Bennett, K. L., Funk, M., Tschernutter, M., Breitwieser, F. P., Planyavsky, M., Mohien, C. U., . . . Schmidt-Erfurth, U. (2010). Proteomic analysis of human cataract aqueous humour: Comparison of one-dimensional gel LCMS with two-dimensional LCMS of unlabelled and iTRAQ®-labelled specimens. *Journal of Proteomics, 74*(2), 151-166.

Bumbrah, G. S., & Sharma, R. M. (2016). Raman spectroscopy – Basic principle, instrumentation and selected applications for the characterization of drugs of abuse. *Egyptian Journal of Forensic Sciences, 6*(3), 209-215.

Burns, D. A., & Ciurczak, E. W. (2007). *Handbook of Near-Infrared Analysis*. Boca Raton, FL: CRC Press.

Butler, H. J., Ashton, L., Bird, B., Cinque, G., Curtis, K., Dorney, J., . . . Martin, F. L. (2016). Using Raman spectroscopy to characterize biological materials. *Nat Protoc, 11*(4), 664-687. doi:10.1038/nprot.2016.036

Camo Analytics. (2020). Modeling, prediction and optimisation. Retrieved from https://www.camo.com/unscrambler/

Chalmers, J. M., Edwards, H. G. M., & Hargreaves, M. D. (2012). *Infrared and Raman spectroscopy in forensic science* (1 ed.). United Kingdom: John Wiley and Sons Ltd.

Chen, K. H., Cheng, W. T., Li, M. J., & Lin, S. Y. (2006). Corneal calcification: chemical composition of calcified deposit. *Graefes Arch. Clin. Exp. Ophthalmol, 244*, 407-410.

Clemens, G., Hands, J. R., Dorling, K. M., & Baker, M. J. (2014). Vibrational spectroscopic methods for cytology and cellular research. *Analyst, 139*, 4411–4444.

Cobarg, C. C. (1995). *Physikalische Grundlagen der wassergefilterten Infrarot-A-Strahlung*. Stuttgart: Grundlagen und Anwendungsmöglichkeiten.

Colourbox. (2020). Science Electromagnetic Spectrum diagram illustration. In (Vol. 54,36 x 22,06 cm at 300 dpi 1.6 MB).

Domon, B., & Aebersold, R. (2006). Mass spectrometry and protein analysis. *Science, 312*(5771), 212–217.

Duan, X., Lu, Q., Xue, P., Zhang, H., Dong, Z., Yang, F., & Wang, N. (2008). Proteomic analysis of aqueous humor from patients with myopia. *Mol Vis, 14*, 70-77.

Duindam, J., Vrensen, G., Otto, C., & Greve, J. (1998). Cholesterol, phospholipid, and protein changes in focal opacities in the human eye lens. *Invest. Ophthalmol, 39*, 94-103.
Dunn, M. J. (1986). *Gel Electrophoresis of Proteins*. Oxford: Butterworth-Heinemann.
Eberhardt, K., Stiebing, C., Matthäus, C., Schmitt, M., & Popp, J. (2015). Advantages and limitations of Raman spectroscopy for molecular diagnostics: an update. *Expert Review of Molecular Diagnostics, 15*(6), 773-787. doi:10.1586/14737159.2015.1036744
Evans, J. W., Zawadzki, R. J., Liu, R., Chan, J. W., Lane, S. M., & Werner, J. S. (2009). Optical coherence tomography and Raman spectroscopy of the ex-vivo retina. *J Biophotonics*, 398-406.
Ferraro, J. R., Nakamoto, K., & Brown, C. W. (2003). *Introductory Raman Spectroscopy* (2 ed.). San Diego: Elsevier Science & Technology.
Filik, J., & Stone, N. (2008). Raman point mapping of tear ferning patterns. *Proc. of SPIE, 6853*, 685309-685301.
Freddo, T. F. (2013). A contemporary concept of the blood-aqueous barrier. *Prog Retin Eye Res, 32*, 181-195. doi:10.1016/j.preteyeres.2012.10.004
Gellermann, W., & P. S. Bernstein. (2004). Noninvasive detection of macular pigments in the human eye
J Biomed. Opt, 9, 75-85.
Ghose, T., Qiugley, J. H., Landrigan, P. L., & Asif, A. (1973). Immunoglobulins in aqueous humour and iris from patients with endogenous uveltis ancd patients with cataract. *Brit. J Ophthal, 57*, 897.
Gómez, D. A., Coello, J., & Maspoch, S. (2019). The influence of particle size on the intensity and reproducibility of Raman spectra of compacted samples. *Vibrational spectroscopy, 100*, 48-56.
Harrison, J. F. (2009). Wavenumbers. Retrieved from https://www2.chemistry.msu.edu/faculty/harrison/cem483/
Hofko, B., Alavi, M. Z., Grothe, H., Jones, D., & Harvey, J. (2017). Repeatability and sensitivity of FTIR ATR spectral analysis methods for bituminous binders. *Materials and Structures, 50*(3), 187. doi:10.1617/s11527-017-1059-x
Hosseini, K., Jongsma, F., Hendrikse, F., & Motamedi, M. (2003). Non-invasive monitoring of commonly used intraocular drugs against endophthalmitis by Raman spectroscopy. *Lasers Surg. Med, 32*, 265-270.
Hou, P. Y., Mougin, J., Ager, J. W., & Galerie, A. (2011). Limitations and Advantages of Raman Spectroscopy for the determination of oxidation stresses. *ResearchGate*.
Hulka, B. S. (1990). *Overview of biological markers. In: Biological markers in epidemiology*. New York: Oxford University Press.
Ikeuchi, K., & Sato, K. (1991). Determining Reflectance Properties of an Object Using Range and Brightness Images. *IEEE Transactions on Pattern Analysis and Machine Intelligence, 13*, 1139-1153. doi:10.1109/34.103274
Izzotti, A., Longobardi, M., Cartiglia, C., & Saccà, S. C. (2010). Proteome alterations in primary open angle glaucoma aqueous humor. *J Proteome Res., 9*(9), 4831-4838.
Jones, R. R., Hooper, D. C., Zhang, L., Wolverson, D., & Valev, V. K. (2019). Raman Techniques: Fundamentals and Frontiers. *Nanoscale Ress Lett, 14*, 231. doi:10.1186/s11671-019-3039-2
Kaufman, P. L., & Alm, A. (2003). *Adler's Physiology of the Eye*: Mosby Inc.
Kitagawa, T., & Hirota, S. (2002). *Raman Spectroscopy of Proteins* (Vol. 5). New Jersey: John Wiley & Sons.
Klenkler, B., & Sheardown, H. (2004). Review: Growth factors in the anterior segment: role in tissue maintenance, wound healing and ocular pathology. *Exp Eye Res, 79*(5), 677-688.

Kopac, T., & Bozgeyik, K. (2010). Effect of surface area enhancement on the adsorption of Bovine Serum Albumin onto titanium dioxide. *Colloids Surf B Biointerfaces, 76*(1), 265-271. doi:10.1016/j.colsurfb.2009.11.002

Li, C. C., Kuo, M. T., & Chang, H. C. (2010). Review: Raman Spectroscopy – A Novel Tool for Noninvasive Analysis of Ocular Surface Fluid. *Journal of Medical and Biological Engineering, 30*(6), 343-354.

Long, D. A. (2002). *The Raman effect*. Chichester: John Wiley and Sons Ltd.

Mathis, A., Malecaze, F., Bessieres, M. H., Arne, J. L., & Seguela, J. P. (1988). Immunological analysis of the aqueous humour in candida edoohthalmitis. II: Clinical study. *British Journal of Ophthalmology, 72*, 313-316.

Mellerio, J. (1994). *Light effects on the retina*. Philadelphia: Saunders.

Merck Life Science AS. (2020). Bovine Serum Albumin solution. Retrieved from https://www.sigmaaldrich.com/catalog/product/sial/a4628?lang=en&region=NO

Movasaghi, Z., Rehman, S., & Rehman, I. (2007). Raman Spectroscopy of Biological Tissues. *Applied Spectroscopy Reviews, 42*, 493-541. doi:10.1080/05704920701551530

Munson, C. A., L.Gottfried, J., Jr, F. C. D. L., McNesby, K. L., & Miziolek, A. W. (2007). *Counterterrorist Detection Techniques of Explosives*.

Murray, P. I., Hoekzema, R., Luyendi, L., Konings, S., & Kijlsrra, A. (1990). Analysis of Aqueous Humor Immunoglobulin G in Uveifis by Enzyme-Linked Immunosorbenf Assay, Isoelecfric Focusing, and Immunoblotting. *Investigative Ophthalmology & Visual Science,, 31*, 10.

Nano Photon. (2020). Basic of Raman scattering. Retrieved from https://www.nanophoton.net/raman-spectroscopy/lessons/lesson-1

Nobel Prize. (2020). The Nobel Prize in Physics 1930. Retrieved from www.nobelprize.org/prizes/physics/1930/summary

Noel, J. C. B., Massoud, M., Fred, H., & James, P. W. (2005). Remote temperature monitoring in ocular tissue using confocal Raman spectroscopy. *J. Biomed. Opt, 10*.

Ohashi, Y., Dogru, M., & Tsubota, K. (2006). Laboratory findings in tear fluid analysis. *Clin Chim Acta, 369*(1), 17-28. doi:10.1016/j.cca.2005.12.035

Parachalil, D. R., Brankin, B., McIntyre, J., & Byrne, H. J. (2018). Raman spectroscopic analysis of high molecular weight proteins in solution - considerations for sample analysis and data pre-processing. *Analyst, 143*(24), 5987-5998. doi:10.1039/c8an01701h

Pavlina2.0. (2006). Raman energy levels. Retrieved from https://commons.wikimedia.org/wiki/File:Raman_energy_levels.jpg

Pelletier, C. C., Lambert, J. L., & Borchert, M. (2005). Determination of glucose in human aqueous humor using Raman spectroscopy and designed-solution calibration. *Appl. Spectrosc, 59*, 1024-1031.

Rajagopalan, P., Advani, J., Pinto, S. M., & Goel, R. (2015). Proteomics of Human Aqueous Humour. *Omics: a journal of integrative biology, 19*(5), 283-293. doi:10.1089/omi.2015.0029

Ramírez-Elías, M. G., & González, F. J. (2018). Raman Spectroscopy for In Vivo Medical Diagnosis. *intechopen*. doi:10.5772/intechopen.72933

Reed, G. F., Lynn, F., & Meade, B. D. (2002). Use of coefficient of variation in assessing variability of quantitative assays. *Clinical and diagnostic laboratory immunology, 9*(6), 1235-1239. doi:10.1128/cdli.9.6.1235-1239.2002

Reyes-Goddard, J. M., Barr, H., & Stone, N. (2008). Surface enhanced Raman scattering of herpes simplex virus in tear film. *Photodiagnosis Photodyn Ther, 5*, 42-49.

Richardson, M. R., Price, F. W., Pardo, J. C., Grandin, J. C., You, J., Wang, M., & Yoder, M. C. (2009). Proteomic analysis of human aqueous humor using multidimensional protein identification technology. *Molecular Vision, 15*, 2740-2750.

Sebag, J., Nie, S., Reiser, K., Charles, M., & Yu, N. (1994). Raman spectroscopy of human vitreous in proliferative diabetic retinopathy. *Invest Ophthalmol. Vis. Sc, 35*, 2976-2980.

Sen, D. K., Sarin, G. S., & Saha, K. (1977). Immunoglobulins in human aqueous humour. *Br J Ophthalmol, 61*(3), 216–217.

Settle, F. A. (1997). *Handbook of instrumental techniques for analytical chemistry*. New Jersey: Prentice Inc.

Siebinga, I., Vrensen, G., Otto, K., Puppels, G., Mul, F. D., & Greve, J. (1992). Ageing and changes in protein conformation in the human lens: a Raman microspectroscopic study. *Exp. Eye Res, 54*, 759-767.

Stewart, S., & Fredericks, P. M. (1999). Surface-enhanced Raman spectroscopy of amino acids adsorbed on an electrochemically prepared silver surface. *Spectrochim. Acta A Mol. Biomol. Spectro, 55*(7-8), 1641–1660.

Tamhane, M., Cabrera-Ghayouri, S., Abelian, G., & Viswanath, V. (2019). Review of Biomarkers in Ocular Matrices: Challenges and Opportunities. *Pharmaceutical Research, 36*(40).

Tkachenko, N. V. (2006). *Optical Spectroscopy: Methods and Instrumentations*.

Wells, G., Prest, H., & Russ, C. W. (2011). Signal, Noise, and Detection Limits in Mass Spectrometry. *Agilent Technologies*.

Wiese, S., Reidegeld, K. A., Meyer, H. E., & Warscheid, B. (2007). Protein labeling by iTRAQ: A new tool for quantitative mass spectrometry in proteome research. *Proteomics, 7*(3), 340–350.

Wilkins, M. R., J. C. Sanchez, Gooley, A. A., Appel, R. D., Humphery-Smith, I., & Hochstrasser, D. F. (1996). Progress with proteome projects: why all proteins expressed by a genome should be identified and how to do it. *Biotechnology and Genetic Engineering Reviews, 13*(1), 19-50.

Willard, H. H., Meritt, L. L. J., Dean, J. J., & Settle, F. A. J. (1988). *Instrumental methods of analysis* (7 ed.). New Delhi: CBS Publisher & Distributors.

Xiang, M., Zhang, X., Li, Q., Wang, H., Zhang, Z., Han, Z., . . . Chen, X. (2017). Identification of proteins in the aqueous humor associated with cataract development using iTRAQ methodology. *Molecular Medicine Reports*, 3111-3120. doi:10.3892/mmr.2017.6345

Zhao, J., Lui, H., McLean, D. I., & Zeng, H. (2010). Real-time raman spectroscopy for noninvasive in vivo skin analysis and diagnosis. In: New Developments in Biomedical Engineering. *InTech*.

List of tables, figures and formulae

Abbreviations

BSA: Bovine Serum Albumin

HSA: Human Serum Albumin

AH: Aqueous humor

hAH: Human aqueous humor

SNV: Standard Normal Variate

DCDRS: Drop Coating Deposition Raman Spectroscopy

SERS: Surface-enhanced Raman spectroscopy/Scattering

CRM: Confocal Raman microscopy

FTIR: Fourier transform infrared

FT: Fourier Transform

ELISA: Enzyme-linked immunosorbent assay

SDS-PAGE: Sodium Dodecyl Sulfate-Polyacrylamide Gel Electrophoresis

2-DE: Two-Dimensional gel Electrophoresis

2D-DIGE: Two-Dimensional Differential Gel Electrophoresis